# Analysis of Strength Variation in Glass Due to Ion Exchange

Andrew Kulp

Thesis submitted to the faculty of the Virginia Polytechnic Institute and State University in partial fulfillment of the requirements for the degree of Master of Science in the Department of Materials Science and Engineering

David Clark

Gary Pickrell

Carlos T. A. Suchicital

May 21, 2012

Blacksburg, Virginia

Keywords: Fractography, Glass, Ion Exchange, Statistical Analysis, Strength, Weibull Analysis

# Analysis of Strength Variation in Glass Due to Ion Exchange

**Andrew Kulp**

## Abstract

The main goal of this project was to compare the changes in statistical variation and Weibull characteristics of the strength of glass rods as modified by heat treatment with and without an ion exchange bath. Several sample groups of 30 sodium borosilicate glass rod specimens were heat treated at various temperatures in air and in a potassium nitrate salt bath to induce an ion exchange process. All samples were then tested to failure in 4-point bending to assess the resulting Modulus of Rupture (MOR). Statistical analysis techniques and Weibull analysis were used to study the variations which occur within and between strength distributions of each sample group. A smaller sampling of test groups was subjected to fractographic analysis to study the effect of ion exchange on fracture features. The data shows that the ion exchange process caused a statistically significant increase in the strength of the glass rods. Samples which were heat treated do not show any significant changes in average strength. The fractographic analysis suggests that no changes in fracture morphology occurred as a result of ion exchange process, and that the critical flaw size population was not significantly different.

## Dedication

This thesis is dedicated to those loyal and loving people who supported me through my entire academic career. These people most definitely include my family, my beautiful girlfriend Lauren Robbins, and my wonderful friends (both from high school and college). Thank you all for helping me through this long and arduous journey.

## Acknowledgements

I would like to acknowledge the immense amount of work and support my research group (Ms. Diane Folz, Ms. Marianne Lindsay, Ms. Elizabeth Belcastro, and Dr. Raghunath Thridandapani) put into helping to make this project and thesis come to fruition. I would especially like to acknowledge the many tens (or even hundreds) of hours my advisor, Dr. David Clark, has spent helping me to shape this thesis into its final form. I would also like to thank my defense committee for the insight and wisdom they have given along the course of this project.

**Table of Contents**

**List of Figures**

**List of Tables**

# Chapter 1: Introduction

The ion exchange process is widely known for affecting the strength of glass [1-4]. The goal of this research was to investigate the effect that ion exchange had on the variations in the strength and fracture surface morphology of borosilicate glass rods.

Several objectives were required to reach this goal:

1. Develop an ion exchange process which will improve the strength of a commercial sodium borosilicate glass.
2. Employ methods of statistical analysis to evaluate variations in average strength and the strength distribution due to ion exchange.
3. Conduct a Weibull analysis to investigate variations in characteristic strength and Weibull modulus (reliability) as a result of the ion exchange process.
4. Determine, by means of fractography, if similar fracture surface features exist on the glass samples which have been treated using ion exchange as on as received samples, and, if so, determine if these features conform to different models.

# Chapter 2: Background Information

## Glass Production

Glass is a widely used term which can refer to any solid which lacks long range structural periodicity[1]. A wide range of materials can be used to form a glass, but the most widely known glass material is that which is composed of a silicon dioxide (silica) matrix. Silica glasses can be pure or composed of silica with small

percentages of other materials, which include but are not limited to alkalis, boron, aluminum, calcium, or lead. Silica glass is used in construction, consumer products, electronics and many other applications. Pure fused silica glass is known for its high temperature stability, low thermal expansion and high resistance to thermal shock, and high chemical durability. This combination of properties can be manipulated as needed and other properties improved by adding small amounts of raw materials to the matrix[1, 2, 5].

Most glasses are manufactured on a temperature-time schedule such as the one shown in Figure 2.1. Raw materials are added to the furnace in the form of carbonates and oxides and heated above their melting points[1, 2, 5]. The molten material remains in the furnace for a sufficient time to achieve homogenization (10-15 hours), and is then cast or drawn to achieve the final shape[6]. This forming operation is very rapid and can result in a buildup of internal stress for large cross-sectioned products[5]. Thus an annealing step is usually required to reduce the stress and produce a glass product that is safe to use. The annealing process is carried out at a sufficiently high temperature (400 to 500°C) to release the stresses in a few hours or less. The process, from melting to annealing, can take from 10 to 20 hours, depending on the composition and final form (container, rod, tube, etc.).

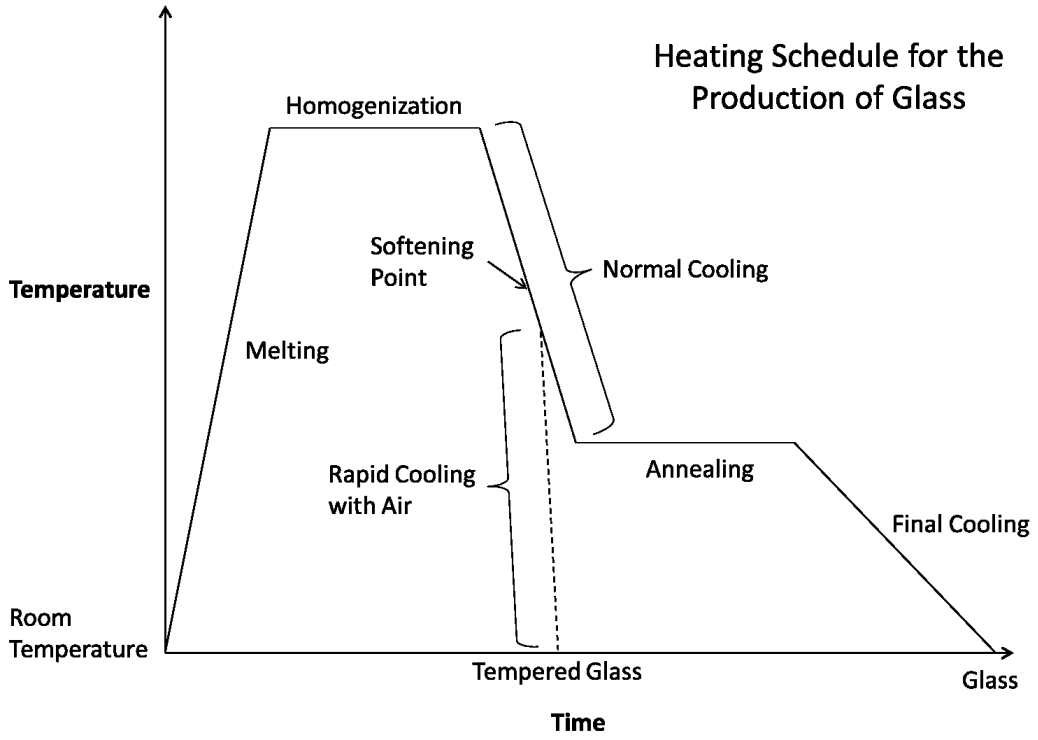


Figure 2.1: A schematic representation of an example of a heating schedule required to produce silicate glasses.

Also shown in Figure 2.1 is the method for manufacturing tempered glass. Slightly below the softening point, the surface of the glass is cooled very rapidly with air resulting in a glass that can be ten times stronger than annealed glass. This process requires a lot of control and can only be accomplished in fairly simple shapes (i.e. plate glass) with thick cross sections[1, 5]. As discussed later in this chapter, ion exchange is another method for enhancing strength in thinner and more complex shaped glass products.

Based upon the bonding energies of silicon and oxygen, pure silica glass should have a much higher strength than that which is observed[5]. When network modifiers such as sodium oxide ($Na_2O$) are added to reduce the processing temperature, the theoretical strength is reduced but still much higher than what is

observed in practice. So, what causes the measured or practical strength of glass to be so much lower than the theoretical value? Based on the work of Inglis and Griffith, it is now well established that sharp tipped flaws (also known as Griffith flaws) are present in the surface of all glass (due to manufacturing and handling) and these flaws act as stress-raisers when loads are applied (see Figure 2.2)[7, 8].

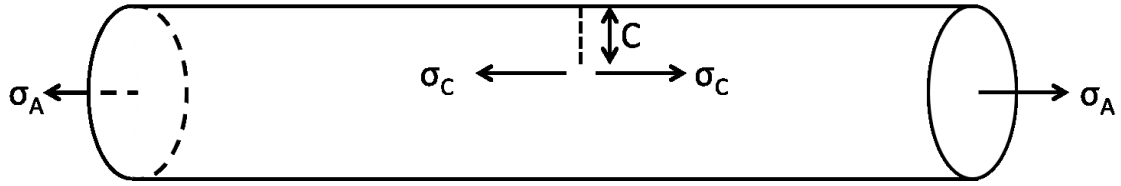


Figure 2.2: A schematic drawing of a Griffith's type flaw of length ***C*** and the effect which stress on bulk, $\boldsymbol{\sigma_A}$, has on the stress at the crack, $\boldsymbol{\sigma_C}$.

When a load is applied resulting in a stress, $\boldsymbol{\sigma_A}$, the stress at the flaw tip, $\boldsymbol{\sigma_C}$, is substantially greater as shown in Equation 2.1 [9].

$$\sigma_C = 2\sigma_A \left(\frac{C}{a_0}\right)^{1/2} \tag{2.1}$$

Where ***C*** is the flaw length and $\boldsymbol{a_0}$ is the flaw tip radius which is assumed to be equal to half the interatomic spacing (~$10^{-4}$ μm). From the equation it can be seen that the stress at the tip of a sharp flaw that is 1 μm in length can be 200 times greater than the applied stress, $\boldsymbol{\sigma_A}$. When the applied stress causes $\boldsymbol{\sigma_C}$ to exceed the theoretical strength, failure will occur and the measured strength, $\boldsymbol{\sigma_m}$, is equal to $\boldsymbol{\sigma_A}$. Values of ***C*** from literature have been found to range from 1 μm to 100 μm [9]. Assuming that the glass has a theoretical strength of 20,000 MPa and a flaw size, ***C***, of 1 μm, the measured strength of the glass would be about 100 MPa. If ***C*** is increased to a length of 50 μm the measured strength of the glass would be 28

MPa. Considering the uncertainties in theoretical strength, dimension of the crack tip radius, and geometry of the crack, the measured strength in this study appear to be in agreement with those predicted by Equation 2.1.

Since the population of flaw size can vary significantly depending on the conditions to which the glass has been subjected, the measured strength will vary in a similar fashion[5]. When a homogeneous stress is applied such as that shown in Figure 2.2, the fracture will always nucleate at the largest flaw size (also referred to as the *critical* flaw). Any treatment that will reduce the flaw size, $\boldsymbol{C}$, or increase the tip radius, $\boldsymbol{a_0}$, will increase the measured strength of the glass [1, 4, 5, 9]. As discussed later in this chapter, ion exchange has the capability of enhancing glass strength without altering either $\boldsymbol{C}$ or $\boldsymbol{a_0}$. Although the measured strength of the glass is not a constant (because it varies with flaw size), fracture toughness, $\boldsymbol{K_{Ic}}$, is a constant for a given material. Fracture toughness can be determined experimentally using Equation 2.2 [1, 4, 5, 9, 10].

$$K_{Ic} = Y\sigma_m c^{1/2} \tag{2.2}$$

Where $\boldsymbol{Y}$ is a unitless flaw shape factor which, according to the literature, can have a value ranging from approximately 1 to 3.5 based on the type of flaw which is present[9]. $\boldsymbol{K_{Ic}}$ can be obtained by inducing a flaw of known length into the glass and then measuring its strength. The reported fracture toughness for pure silica glass ranges from 0.74 to 0.81 MPa-$m^{1/2}$ and from 0.75 to 0.82 MPa-$m^{1/2}$ for the glass compositions similar to the one used in this investigation[4].

**Surface Modification and Glass Strengthening**

The term *surface modification* can be used for a variety of techniques which involve changing the surface structure and/or composition of glass to improve its strength, fracture characteristics, and chemical durability[4]. These techniques include, but are not limited to, surface abrasion, thermal tempering, and cladding. This thesis employs ion exchange, another form of surface modification, in order to improve the strength of the glass.

Ion exchange strengthening is sometimes referred to as *stuffing*. This term refers to the way in which ions of a larger size than that which are already in the matrix are "stuffed" into the matrix, putting stress on the surrounding atomic bonds[1]. A schematic of stuffing can be seen in Figure 2.3. The ion exchange process was first described by Kistler in 1962 when he noticed a compressive stress as high as 128,000 psi (~900 MPa) could be added by heating soda-lime-silica glass in the presence of $KNO_3$[1]. The induced residual compressive stress in the surface is generally accepted as the mechanism by which the ion exchange process improves the overall strength of the glass.

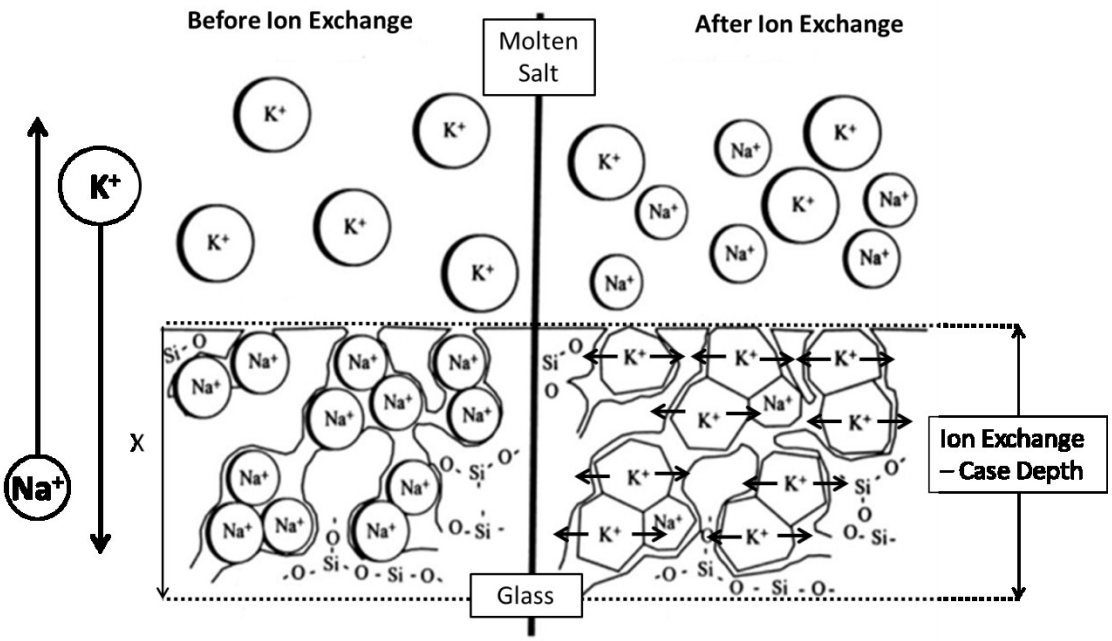


Figure 2.3: A schematic representation of "stuffing" potassium ions into a sodium-silicate glass. Before ion exchange there are no residual stresses in the glass. After ion exchange residual compressive stresses have been developed [11].

In the case of substituting potassium ions for sodium ions in a glass, the potassium ions have a radius of 0.133 nm and the sodium ions have a radius of 0.098 nm[4]. The exchange yields a 36% increase in volume that the silica matrix must accommodate, which it does by compressing its bonds. Since the ion exchange only occurs to a small case depth (depth from the surface into the bulk) the stress translates to a sharp increase in compressive stress at the surface of the glass and a low tensile stress in the center.

Figure 2.4 shows the distribution of stress before and during loading in 4-point bending for an annealed glass specimen (no ion exchange). Before any force is applied there are no significant stresses within the glass. As load is applied the lower half of the glass rod is put into tension and the upper half is put into

compression. With increasing load, the tensile stress increases in magnitude until the ultimate strength of the specimen is reached and causes failure.

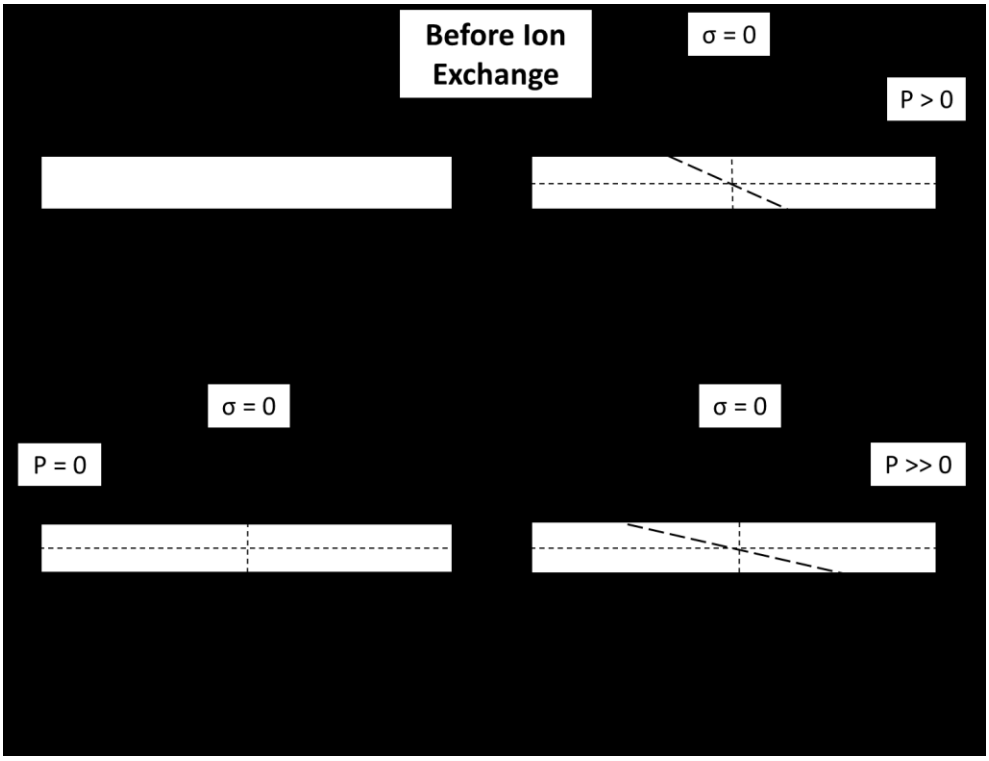


Figure 2.4: (A) a sketch of a glass rod in a 4-point bending test, where P is the applied force. (B) When P=0 there are no residual stresses in the glass rod. (C) When force is applied the upper half of the glass rod is in a compressive stress state and the lower half is in a tensile stress state. (D) As P becomes greater the tensile stress in the lower half increases until failure [12].

This is in contrast to the stress distribution that exists in a glass specimen which has been strengthened via ion exchange. Figure 2.5 shows similar schematics as Figure 2.4; however, when a load is not being applied the specimen is already under a residual stress. The ions which were exchanged put the surface under a high compressive stress, while the bulk of the glass is under a low tensile stress. As force is applied, tensile stresses which build up at the lower surface are negated by the residual compressive stress. Thus, the force must be increased to a greater magnitude in order to reach the ultimate strength of the specimen and cause failure.

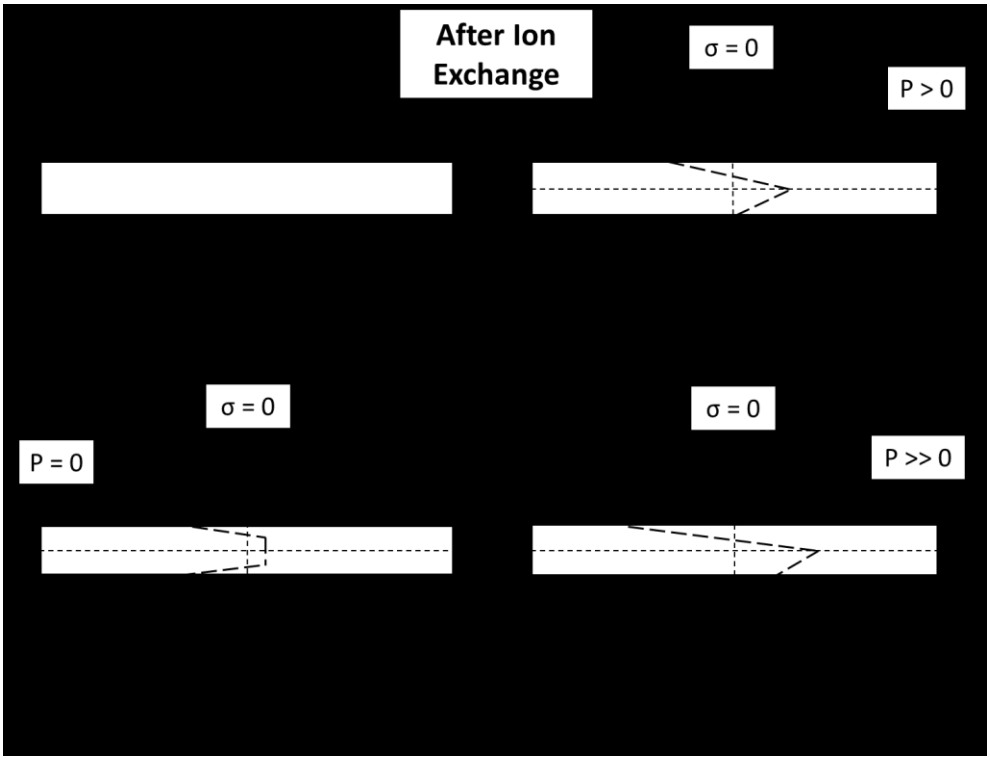


Figure 2.5: (A) a sketch of a glass rod in a 4-point bending test, where P is the applied force. (B) When P=0 there are high residual compressive stresses at both surfaces and low residual tensile stresses in the bulk of the glass rod. (C) When force is applied the upper half of the glass rod is in a compressive stress state and the stress at the lower surface has been negated by the residual compressive stress. (D) As P is increased the tensile stress in the lower half increases until failure[12].

This overall increase in residual compressive stress at the surface due to ion exchange also means an increase of the compressive stress around any flaws which are present in the surface. Figure 2.6 shows the compressive stresses at the flaws work against the applied tensile stress. This inhibits the propagation of cracks from the sharp points of the flaws through the bulk.

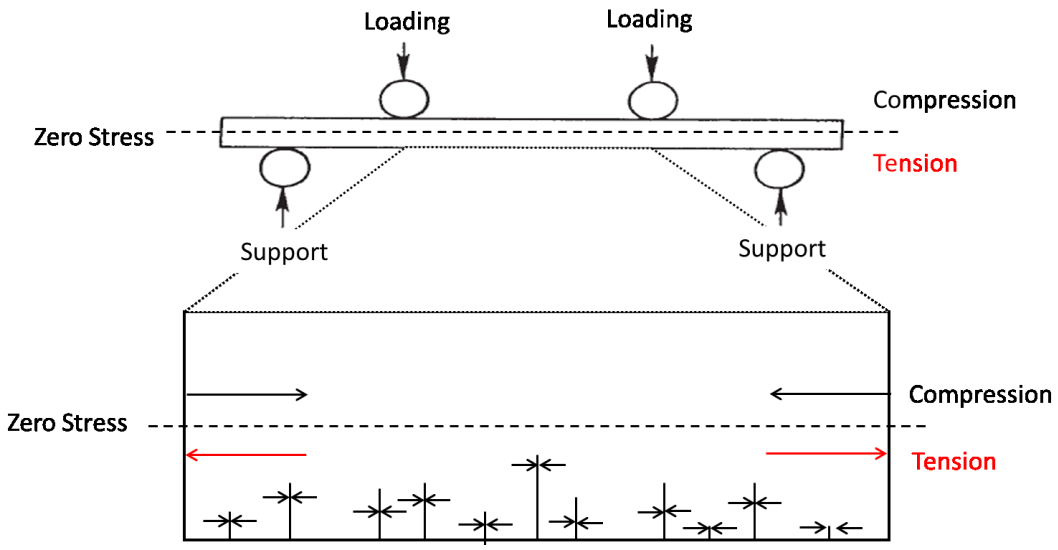


Figure 2.6: A glass rod in 4-point bending showing the difference in stress states between the upper and lower parts of the rod with respect to the applied forces. The region between the loading points has been expanded to show the effect of ion exchange on the flaws at the surface of the glass rod.

Generally, the ion exchange process is carried out in a molten salt bath[1, 4, 5]. Most of these salts are molten around 350°C, but some degrade at around 550°C, so this is a common temperature range (350 to 550°C) for conducting ion exchange. Ion exchange is also time dependent; therefore, the glass may be left in the molten salt bath for up to 24 hours to achieve an adequate increase in strength. The heating schedule for the production of ion exchange strengthened glass is similar to the normal heating schedule (Figure 2.1), but it deviates just after the final cooling step. This can be seen in Figure 2.7.

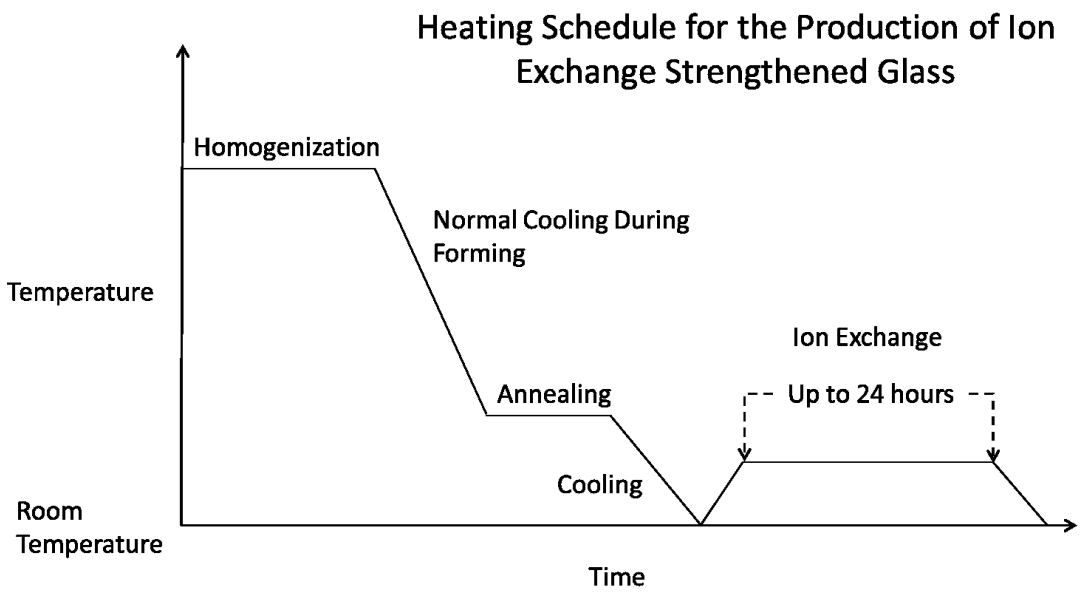


Figure 2.7: A schematic of the heating schedule for the production of ion exchange strengthened glass.

Aside from a molten salt bath, other methods can be used to induce ion exchange. A salt paste, which is an ion exchange salt mixed with an inert carrier agent, such as a clay, can be applied to the glass via dipping or painting [1]. The paste is allowed to dry and then the paste-covered glass is heated and soaked at the desired temperature and time.

Ion exchange is a two-step process. At the interface between the glass and molten salt the two types of alkali ions exchange places with each other (i.e. liquid-surface adsorption) [13]. For example, a sodium ion from the glass will exchange places with a potassium ion from the salt. Once on the glass surface, the potassium ion will move deeper inside the glass and sodium ions move from inside the glass to the surface where they are able to exchange with other potassium ions from the salt. The counter movement of sodium ions to the surface and potassium ions further into the glass is controlled by diffusion and can be mathematically described by Fick's first and second laws [14]. Since the diffusion processes are

much slower than the surface reaction, it is the former that controls the rate of ion exchange. The driving force for diffusion of both types of ions is their concentration gradient. The temperature of the molten salt provides the energy required to overcome any additional energy barriers to ion transport. Since electrical neutrality must be maintained inside the glass the rate of diffusion of ions out of the glass must be equal to the rate of diffusion into the glass. Thus, the ion exchange process is controlled by the slower of the counter diffusing ions.

Of major importance is the depth to which the ion exchange process occurs. The greater the depth, the more effective is the strengthening process and more tolerant is the glass to surface damage. Based on Fick's second law, the depth of ion exchange is dependent on the square root of time, as in Equation 2.3 [14].

$$x = \sqrt{C\ t} \tag{2.3}$$

Where,

***x*** is diffusion distance; the case depth in Figure 2.3;

***C*** is a constant parameter which includes the diffusion coefficient,

***t*** is the time required to reach ***x***.

Due to the square root dependency, using long ion exchange times may not be an effective method of achieving a large case depth.

The Arrhenius relationship in Equation 2.4 gives the temperature dependence of the self-diffusion coefficient [14].

$$D = D_0 e^{-E_a/RT} \tag{2.4}$$

Where,

$\boldsymbol{D}$ is the diffusion coefficient,

$\boldsymbol{D_0}$ is the constant pre-exponential term,

$\boldsymbol{E_a}$ is the activation energy for diffusion per gram mole of diffusing species,

$\boldsymbol{R}$ is the gas constant, and

$\boldsymbol{T}$ is the temperature of the system.

The self-diffusion coefficient describes the diffusion parameters for an individual diffusing species. In a multi-species diffusion process, such as ion exchange, an interdifussion coefficient must be determined. The interdifussion coefficient is analogous to a weighted average of the self-diffusion coefficient of each species. The exponential temperature dependence of the diffusion coefficient indicates that increasing temperature will increase the diffusion depth substantially. However, for the range of temperatures used (350 °C – 550 °C), due to the limitations of the ion exchange salts, the depth of ion exchange is only a few 10's of microns for most commercial glasses.

Besides time and temperature, the composition of the glass and ion exchange species play an important role in the ion exchange process. The ion exchanges usually involve potassium or silver for sodium; or sodium for lithium. Research has shown that alkali-alumina-silicate glasses are the most receptive to the ion exchange process [1]. They allow a high rate of ionic flux, and therefore, require shorter soak times to achieve higher strengths and exchange depths. Borosilicate glasses have been shown to be a less desirable composition for use with ion exchange. Though the process can still be carried out using this composition, it occurs at a slower rate, and yields lower strengths and exchange depths. Glasses with high lead content are not able to be strengthened via ion exchange at all, due

to the low mobility of lead ions at the temperatures this process is carried out at [4].

Ion exchange strengthening has several advantages over tempering. The two main advantages are the ability to strengthen complex shapes and thin cross sectioned products. These advantages allow it to be used in airplane and space vehicle windshields; prescription eye-glass lenses; laboratory glass-ware; and many other consumer products [1]. One of the more high profile consumer products is the Corning line of Gorilla Glass® which, among other things, is used for the glass touchscreens of many smartphones [3]. Gorilla Glass® is one of the most resilient glass products in the consumer market, and it is made possible by a combination of structure and processing technologies one of which includes ion exchange strengthening.

**Statistical and Weibull Analysis**

An important step in designing materials is to verify whether changes made to them have *statistically* significant effects on the properties. Conducting tests in a large sample group allows a distribution of test data to be created [15]. The variations in this distribution can be compared with the variations in the distributions of sample groups with different test parameters. In some cases the arithmetic mean in two different distributions may be exactly the same while having different distributions. The different distributions will most likely result in different performance in the field and in some cases lead to catastrophic failure. This is especially true for brittle materials, such as glass, which typically have wide strength distributions. By comparing the two distributions that difference can be noticed and measured to quantify how dissimilar the two distributions actually are. There are a handful of methods that can be used for this comparison, but two of the

more common ones are an Analysis of Variance (ANOVA) and a *t*-test. Both of these analyses are conducted with a list of assumptions:

- The sample groups are independent of each other;
- The sample groups are drawn from a population with a normal distribution; and
- The variances of the two populations are equal.

If any of these assumptions is false than there may be substantial error in the results of the analyses. According to the Central Limit Theorem any randomly generated sample of averages greater than 30 specimens will follow a normal distribution despite the distribution of the population which the sample averages comes from [15]. However, a population which is heavily skewed may result in a distribution of individual samples which is also skewed even for a sample size greater than 30, and therefore may not follow a normal distribution.

ANOVA is a tool that allows two or more distributions to be compared at once, and takes into account the number of ways the distributions are different [15]. A one-way ANOVA (the type used in this study) takes into account a single varied parameter between all of the distributions, and as different parameters are added the complexity of the ANOVA increases. One of the first steps in performing an ANOVA is to determine the null hypothesis, $H_0$. Commonly, the null hypothesis is that the distributions being compared are all equal. The next step is to perform all of the necessary calculations. The formulas required to calculate a one-way ANOVA are given in Equations 2.5 through 2.8:

$$TSS = \sum_{i,j} y_{ij}^2 - \frac{G^2}{n} \tag{2.5}$$

$$SSB = \frac{\sum T_i^2}{n_i} - \frac{G^2}{n} \tag{2.6}$$

$$SSW = TSS - SSB \tag{2.7}$$

$$F = \frac{s_B^2}{s_W^2} \tag{2.8}$$

Where,

***TSS*** is the Total Sum of Squares,

***SSB*** is the Sum of Squares Between sample groups,

***SSW*** is the Sum of Squares Within the sample groups,

***F*** is the experimental value for the ***F***-test,

$y_{i,j}$ is the ***j***th sample observation selected from population ***i***,

***G*** is the sum of all sample observations,

***n*** is the total sample size,

$T_i$ is the sum of the sample measurements obtained from population ***i***,

$s_B^2$ is ***SSB***/(***t***-1), where ***t*** is the number of sample groups,

$s_W^2$ is ***SSW***/(***n***-1).

The value of the ***F***-statistic is compared with a tabulated critical ***F*** value with a chosen confidence interval $\alpha$ and degrees of freedom, $df = n - 1$ [15]. If the ***F***-statistic is greater than the critical ***F*** value than the null hypothesis is rejected. In the case of the hypothesis stated above, this would mean that *at least* one of the distributions being compared is significantly different from all of the other distributions (with the chosen confidence). There is an obvious drawback to using this analysis, and that is, if the null hypothesis is rejected, you do not know *which* of the distributions that are being compared in the analysis is different from the rest of the distributions.

Another method of evaluating the differences between distributions of data is to perform a pairwise analysis of them using the ***t***-statistic and the Student's ***t***-

distribution to perform a ***t***-test [15]. The ***t***-test takes into account the differences between the arithmetic mean and the differences between the standard variance of the two distributions being compared. As above, the first step in performing a ***t***-test is to form a null hypothesis, $H_0$. Similar to the $H_0$ exemplified above, it would commonly be that the two distributions being compared are exactly equal. The next step is to calculate the ***t***-statistic, which can be done using Equation 2.9.

$$t = \frac{\bar{y}_1 - \bar{y}_2 - D_0}{s_p \sqrt{1/n_1 + 1/n_2}} \tag{2.9}$$

where,

***t*** is the calculated test statistic,

$\bar{\boldsymbol{y}}_{\boldsymbol{1}}$ is the arithmetic mean of sample group 1,

$\bar{\boldsymbol{y}}_{\boldsymbol{2}}$ is the arithmetic mean of sample group 2,

$\boldsymbol{s_p}$ is the standard deviation of the entire sample population,

$\boldsymbol{n_1}$ is the number of samples in sample group 1,

$\boldsymbol{n_2}$ is the number of samples in sample group 2.

The value of the ***t***-statistic is compared with a tabulated critical $\boldsymbol{t_\alpha}$ value with a chosen confidence interval $\boldsymbol{\alpha}$ and degrees of freedom, $\boldsymbol{df} = 2\boldsymbol{n} - 2$, where, ***n*** is the total number of samples in the test [15]. If the calculated absolute value of ***t*** is greater than $\boldsymbol{t_{\alpha/2}}$ (for a two-tailed distribution) than the null hypothesis is rejected. In the case of the hypothesis stated above, this would mean that the two distributions being compared are not equal. The obvious drawback to this analysis is that only two distributions can be compared at once.

By conducting an ANOVA and a ***t***-test analysis on the population of sample groups it is possible to acquire a more complete picture of the differences that exist (or do not exist) between the sample group distributions.

In addition to determining the statistical differences between two different materials it is also important to determine the probability of failure under loading at various stresses. This is especially true for brittle materials such as glass. The strength can be determined by various methods, such as tensile or bending tests. However, considering the possibility for catastrophic failure at any stress it is also useful to determine the probability of failure using a Weibull analysis. A Weibull analysis is conducted by experimentally testing large sample groups of specimens for strength and analyzing the distributions.

The two important reliability characteristics are the Weibull modulus and the unit volume characteristic strength. These characteristics are given in Equations 2.10a, 2.10b, 2.10c, which have been specially adapted for materials data [16]:

$$P_f = 1 - e^{\left[-\int_V^{V_0}\left(\frac{\sigma}{\sigma_0}\right)^m dV\right]} \tag{2.10a}$$

$$\ln\left[\ln\left(\frac{1}{1-P_f}\right)\right] = m\ln\left(\frac{\sigma}{\sigma_0}\right) + \ln\left(\frac{V}{V_0}\right) \tag{2.10b}$$

$$\ln\left[\ln\left(\frac{1}{1-P_f}\right)\right] = m\ln(\sigma - \sigma_0) \tag{2.10c}$$

Where,

$\boldsymbol{P_f}$ is the probability of failure,

$\boldsymbol{V}$ is the unit volume of the experimental specimen,

$\boldsymbol{V_0}$ is the unit volume of the control specimen,

$\boldsymbol{m}$ is the Weibull modulus,

$\boldsymbol{\sigma_0}$ is the unit volume characteristic strength at a failure probability of 63.2%.

$\boldsymbol{\sigma}$ is the experimental MOR.

Equation 2.10b is the result of evaluating the integral and taking the natural logarithm of Equation 2.10a twice. The parameter $\boldsymbol{\sigma}$ is modulus of rupture data which may be derived through 4-point bending tests of the material. This data is ranked in ascending order and given a probability of $n_i/(1+n)$, where $n_i$ is the rank number and $n$ is the number of specimens in the sample group. By adding 1 to the total number of specimens, $n$, $\boldsymbol{P_f}$ is always less than 1, otherwise the denominator of the left side of Equation 2.10b would become equal to 0. The probability of failure increases with increasing stress.

The parameter $\boldsymbol{V_0}$ is equal to the unit volume of the control sample which was originally used to derive the Weibull distribution. The unit volume is the volume of the sample that is under an applied load, for example the volume between the two loading points in a 4-point bending test (as seen in Figure 2.6). In this study, $\boldsymbol{V_0}$ is equal to the unit volume of the glass samples as they are received. $\boldsymbol{V}$ is equal to the unit volume of the experimental sample being evaluated. Since the samples being evaluated are the same volume as the as received samples $\boldsymbol{V} = \boldsymbol{V_0}$. Thus the value of $\boldsymbol{V}/\boldsymbol{V_0} = 1$, and the value of $\ln(\boldsymbol{V}/\boldsymbol{V_0}) = 0$. This being the case, it should be noticed that Equation 2.10b can be written as Equation 2.10c, which is a linear equation and the Weibull modulus, $\boldsymbol{m}$, describes the slope of this line. As the Weibull modulus increases the material can be said to be more reliable since the range of stresses which it will probably fail decreases.

The unit volume characteristic strength, $\boldsymbol{\sigma_0}$, is the stress at which 63.2% of all specimens of the chosen material system and geometry will fail. Given the exact same test conditions, every sample group of the same material system and

geometry will, theoretically, achieve the same unit volume characteristic strength [16, 17].

As mentioned above, a Weibull Analysis must be done with a large group of samples to lower the statistical error. Figure 2.8 shows the expected percent errors of $\boldsymbol{m}$ and $\boldsymbol{\sigma_0}$ as they vary with sample group size for a 90% confidence interval[16].

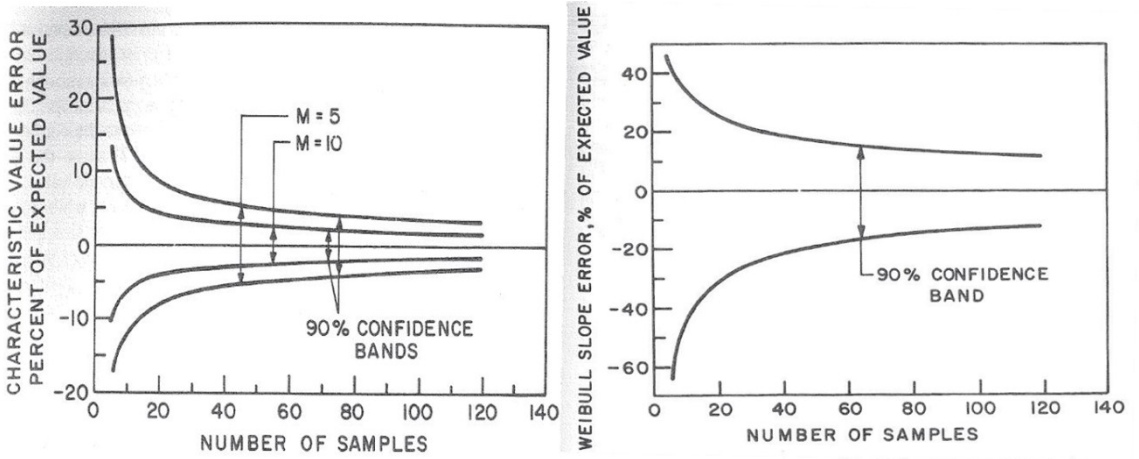


Figure 2.8: The graphed curves show the expected percent error for the unit volume characteristic strength, $\boldsymbol{\sigma_0}$, at a 90% confidence interval as the sample group size varies. The graph shows curves for two different Weibull moduli. The figure on the right depicts the expected percent error for the Weibull modulus, $\boldsymbol{m}$, with a 90% confidence interval as it varies with sample group size [17].

A sample group of 30, for example, would produce approximately 5% and 25% expected error in $\boldsymbol{\sigma_0}$ (when $\boldsymbol{m}$ = 5) and $\boldsymbol{m}$, respectively, with 90% confidence. In most cases, many more than 30 samples are included in the analysis, but 30 (the sample size used in this study) is the recommended minimum [16, 17].

**Fractography**

Fractography is defined as the means and methods for characterizing fractured specimens or components. Fractographic analysis is most useful in describing the failure of highly brittle materials, such as glass, but it can be used to analyze metals

that exhibit low ductility as well. This analysis can be used in two different ways[18].

The first major way that fractography can be used is to reconstruct the circumstances under which a component fails[18]. This includes the stress at failure, the direction and nature of the stress, and the position and size of the critical flaw. This information can be used to engineer future components to serve better as well as to improve the ability to tell when a component will fail. The second way fractography can be used is in the laboratory. Specimens are broken under a controlled manner with every aspect of the applied stress being known [18]. The fracture surfaces are examined to correlate the fracture characteristics with each aspect of the applied stress [10, 18, 19]. Analysis of the fracture surfaces of a broken specimen can be used to describe nearly every characteristic of the the nucleation and propagation of a crack. The fundamentals of fractography involve identifying key features which are signs of different aspects of crack propagation.

Referring to Figure 2.2, when the applied stress, $\boldsymbol{\sigma_A}$, is such that $\boldsymbol{\sigma_c}$ is equal to the theoretical strength of the glass the flaw begins to propagate through the glass. The flaw propagation proceeds slowly at first and then picks up speed until complete fracture occurs[5, 10]. The propagating flaw and its interaction with the acoustic wave that it generates results in some well-defined features on the fracture surface, as seen in Figure 2.9.

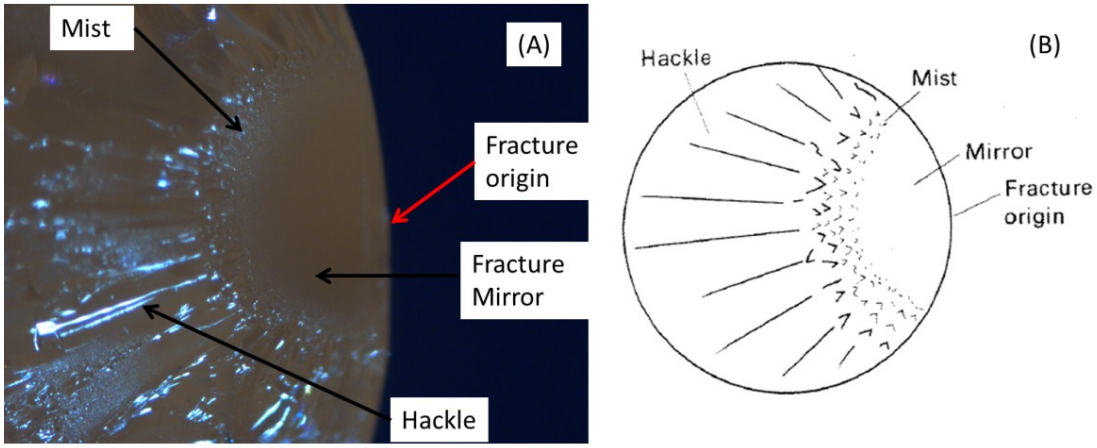


Figure 2.9: A) A micrograph of a fractured glass rod. B) A pictorial representation illustrating the various fracture surface features.

The fracture surface consists of four distinct features [5, 10, 18, 19]:

1. The original flaw leading to fracture (fracture origin);
2. A smooth region referred to as the mirror surface;
3. A region where the smooth surface begins to roughen referred to as mist; and
4. A very rough surface due to crack branching referred to as hackle.

It can be seen that the hackle region is composed of striations that "point" to the original flaw. Similar surface morphology can be found on glass specimens fractured in tension or bending tests. However, as will be discussed later in this section, samples broken in bending tests have some unique features of their own.

As previously mentioned the mirror is a result of the slow crack propagation just after it nucleates [5, 10, 18, 19]. The mist appears as a result of accelerating crack propagation with increasing stress. As the crack propagation accelerates away from the fracture origin, the level of the stress slowly decreases. As the velocity of cracking nears its terminal velocity the surface appears as mist. At the point where

terminal velocity is reached, the hackle begins, and the crack bifurcates into a series of many more cracks.

In samples fractured in uniaxial tension, as in Figure 2.10, the crack propagates in a direction away from the plane of the fracture origin cleaving the sample into three pieces [5]. Two of the pieces contain the two fracture surfaces which resulted from the initial crack, the third is a crescent shaped wedge created by the propagation of the crack away from the plane of initial fracture.

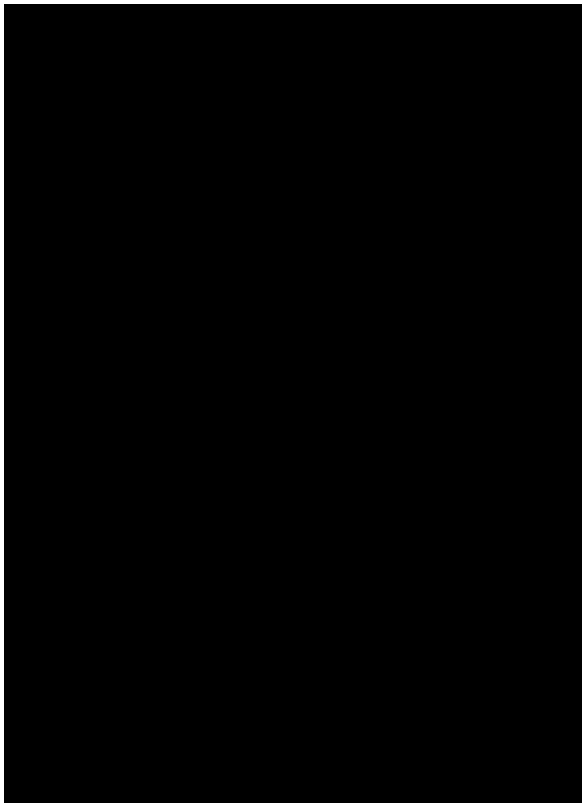

Figure 2.10: A pictorial representation of a glass rod which has been broken in uniaxial tension [5].

In contrast with this type of failure, a specimen which has failed in bending (the test used in this study) shows a slightly different type of fracture. Figure 2.4 illustrates the distribution of the stress on a specimen in bending[18]. The tensile stresses cause a crack to nucleate at the critical flaw, and as the crack propagates

through the thickness of the sample the tensile stress decreases and the compressive stress increases. As shown in Figure 2.11, the crack begins to curve in order to align itself parallel to the compressive stress at the upper surface of the rod. Thus, the crack propagates in such a way as to remove the effect of the compressive stress on its ability to continue propagating. This feature is known as a compression curl or cantilever curl.

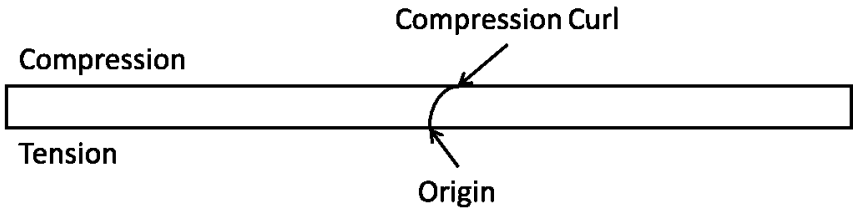


Figure 2.11: A pictorial representation of a glass specimen fractured in bending.

It has been shown that there is an inverse relationship between the applied failure stress, $\sigma_m$, and the radius of the mirror surface, $r$ [5, 10, 18, 19]. The value of the mirror constant in Equation 2.11 depends on the glass composition. What is not clear is how the value is affected by strengthening mechanisms such as tempering and ion exchange. Also, note the similarity of Equation 2.11 to Equation 2.2 which shows the relationship between the original flaw size and measured strength.

$$\sigma_m \sqrt{r} \cong Constant \tag{2.11}$$

Crack features such as fracture origin, mirror, mist, and hackle are useful in measuring the size of the critical flaw at which the fracture originated [5, 10, 18, 19]. The critical flaw size can be used to determine the stress that was being applied at the moment just before crack nucleation. Commonly, the critical flaw size is difficult to measure in practice. In these cases, the fracture toughness, $K_{Ic}$, and measured strength can be used with Equation 2.2 to calculate an approximation

of the critical flaw size, ***C***, assuming a value of 1 for the crack shape parameter, ***Y***. The value of 1 was selected for convenience since the actual shape of the flaw is not known. This should not make a significant difference in the results since all samples are likely to have the same flaw geometry. The ratio of the fracture mirror radius to the critical flaw size has been found to be constant within a material [9]. The ratio reported is 12.5 for fused silica and 10.0 for borosilicate glass [9].

When taken from many samples, the measurements of the fracture features which lead to failure can be useful in explaining changes in measured strength. Using information about the flaw population that exists in a given material can allow engineers to vary composition, processing, and handling procedures of that material to reduce the population of the critical flaw size that results in failure below the desired stress level.

## Chapter 3: Experimental Procedures

### Materials Selection and Sample Preparation

The glass composition selected for this study is referred to as a sodium borosilicate glass. These glasses are comprised of about 20 wt% sodium oxide ($NaO_2$), and varying percentages of boron oxide ($B_2O_3$) and silica ($SiO_2$) [2]. Boron oxide occurs in a triangular coordination within the silica matrix, and the sodium ions occur as bridging connections between oxygen ions in a tetrahedral silica formation. The resulting structure is a random network of silica tetrahedra with intermittent boron-oxygen and oxygen-sodium bonds.

The lower coordination number of the $B_2O_3$ groups and the structure-disrupting nature of the sodium ions in the silica matrix lower the viscosity of the glass matrix

as compared with the viscosity of pure silica [2]. The lower viscosity also lowers the glass transition temperature. Borosilicate glasses, in general, have lower thermal expansion and better resistance to thermal shock compared with silica glass. They also have improved chemical durability. These properties make them useful as headlamps for automobiles, glass cook ware, and glass-ware for laboratories.

The AR-Glas® borosilicate glass system, made by SCHOTT™, was chosen because of its high sodium composition, which should facilitate ion exchange strengthening. Full details on the composition and properties of the AR-Glas® materials system are available in Appendix A. The samples were received as rods with a 6 mm nominal diameter and 1500 mm in length.

The glass rods were sectioned to roughly 100 mm lengths using a pipe cutter to score the circumference of the rod until the rod broke in two. The sectioned rods were kept together in a plastic sample container maintained at about 65°F to 75°F with no humidity control. All samples were kept this way for no more than 1 to 2 weeks before being tested for strength in bending.

**Heat Treatment Sample Preparation**

Randomly chosen as received samples; which were sectioned and stored as described above; were placed along the floor of a stainless steel pan of about 1 millimeter in thickness. Thirty samples were treated at one time. The pan was centered on the floor of the furnace and was not covered. A thermocouple was wrapped around one of the glass rod samples to monitor the temperature of the glass during heating. This setup can be seen in Figure 3.1. The heating schedule consisted of a ramp of 5 °C/min. up to the specified glass temperature. The furnace

was held at a specified temperature for 15 minutes before being allowed to oven cool. The temperatures and times are included in Chapter 4.

Figure 3.1: A mock-up of the placement of the glass rods in a steel pan in a furnace with thermocouple attached to one rod.

**Ion Exchange Sample Preparation**

The chemical modification material chosen was potassium nitrate ($KNO_3$) which comes in the form of a coarsely ground powder. Figure 3.2 shows the floor of a stainless steel pan (same as that used for the heat treatments) was covered with a thin layer of potassium nitrate salt and then 30 randomly chosen as received samples, cut and stored as described above, were placed in the pan on top of the thin layer of $KNO_3$. In order to ensure that the glass samples were completely covered when the $KNO_3$ melted, the samples were covered with another, thicker layer of potassium nitrate, as can be seen in Figure 3.3. The pan was placed in the center of the furnace floor and covered with a plate of refractory in order to reduce the temperature differential between the glass, salt and air, as shown in Figure 3.4. A thermocouple was wrapped around one of the samples in order to monitor the temperature, as shown in Figure 3.1. The heating schedule consisted of a ramp of 2.5 °C/min. up to a glass temperature of 350 °C. The heating rate was decreased

compared with the heat treatment in order to account for the mass of the ion exchange salt. The furnace was held at that temperature for either 15 or 30 minutes before being allowed to oven cool.

Figure 3.2: A mockup of glass rods on a bed of potassium nitrate salt in a steel pan.

Figure 3.3: A mockup of glass rods covered in potassium nitrate salt in a steel pan.

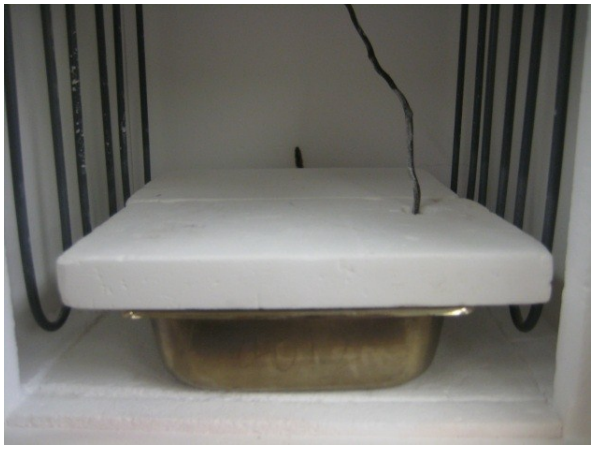

Figure 3.4: A mockup of the steel pan; with glass rods and potassium nitrate inside, and a thermocouple in contact with the glass rods; inside a furnace.

Once the oven was completely cool the pan was removed from the oven and the samples were removed from the salt. The rods were rinsed thoroughly and soaked in room temperature water in a sonic cleaner for approximately 10 minutes. Once dry the samples were stored in the same container as the rest of the samples.

**Materials Characterization**

The effectiveness of the ion exchange process was evaluated through two main characterization methods. The first method was through evaluating the bending strength of the glass rods, and the second method utilized microscopy and fractography to evaluate changes in the fracture surface morphology of the glass rods.

All strength evaluations were done using a ComTen 95T testing stand with a 2000 lb (8896 N) load cell and 4-point bending test jig. The data was gathered using the ComTen Acquisition Program which was provided with the testing stand. The testing stand can be seen in Figure 3.5. The results of the tests were recorded as peak load values at failure. Each group of 30 samples was completed in a testing session to help minimize error due to testing procedures.

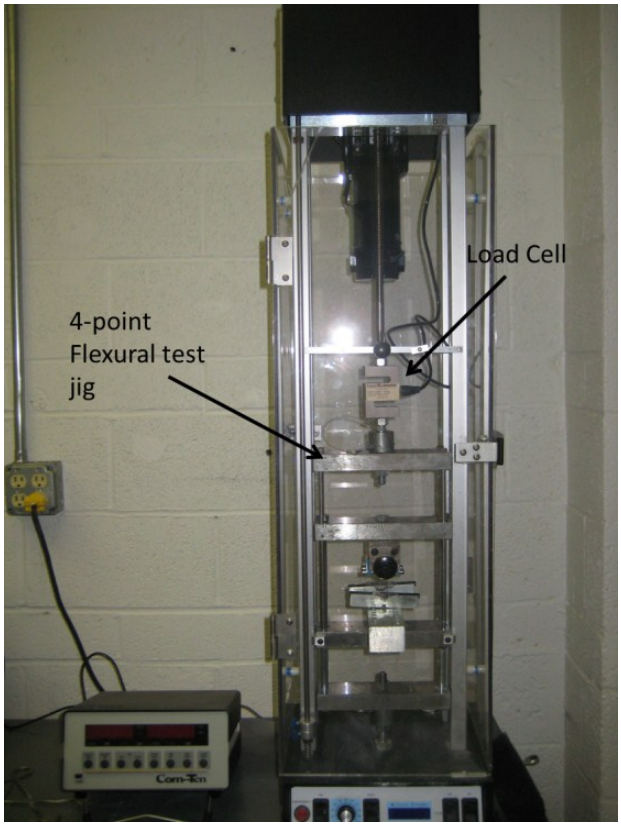


Figure 3.5: The ComTen 95T test stand with load cell and a 4-point bending test jig.

The strength test was performed using a standard 4-point bending test jig and in concordance with ASTM standards[20]. Figure 3.6 (also refer to Figure 2.6) shows the 4-point bending test jig with loading points and support points labeled. The loading span was measured from one loading point to the other loading point, and the support span was measured from one support point to the other support point. The support span was 75 mm, the loading span was 22 mm, and the displacement rate was approximately 1.5 mm/min for all samples. All samples were left unabraded for the bending test. A small piece of polymer putty was used on each support point to hold the glass rods in position.

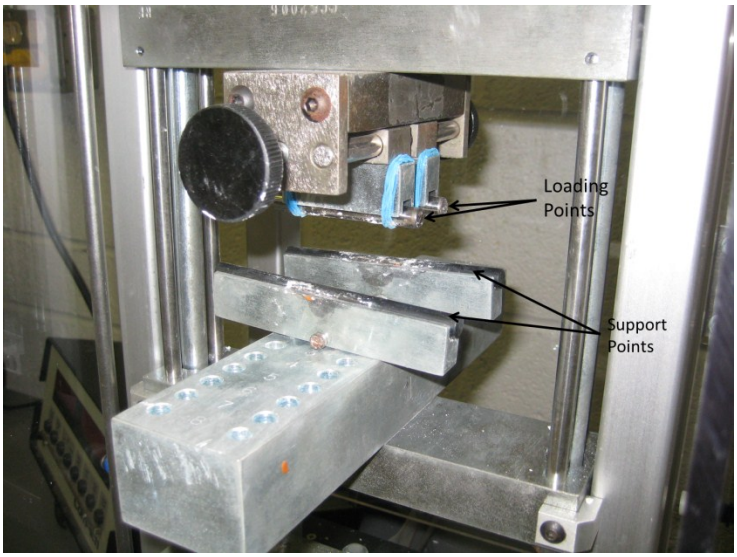


Figure 3.6: A 4-point bending test jig with loading points and support points labeled.

The samples analyzed via fractography were not the same as those used for the statistical and Weibull analysis. Although fewer samples (5 in each group) were used for the former, the testing procedures were the same as those used for statistical and Weibull analysis.

Prior to being subjected to the 4-point bending tests samples were prepared for fractographic analysis. The black markings on the glass rod, which can be seen in Figure 3.7, designate the loading points and serve to allow the specimen to be reconstructed after fracture. A marking on the glass rod at one of the support points, as seen in Figure 3.8, also helps to distinguish the two halves of the specimen after fracture[18, 21]. Tape was applied only to the top half of the specimen, since this is the region that will be placed under compressive stress when in loading it will not interfere with the test. The tape is not expected to interfere with the tests and aids in reconstruction of the fractured specimen. The bending test apparatus was prepared by covering the supporting structure with a soft fibrous material, as can be seen in Figure 3.8. The soft material further reduces

the chance of secondary fractures occurring due to pieces of the fractured specimen hitting the apparatus with a high energy. The material also kept fragments from scattering too profusely. The area within the testing chamber, below the bending test jig, was kept free of debris prior to each test to aid in gathering any scattered fragments after fracture.

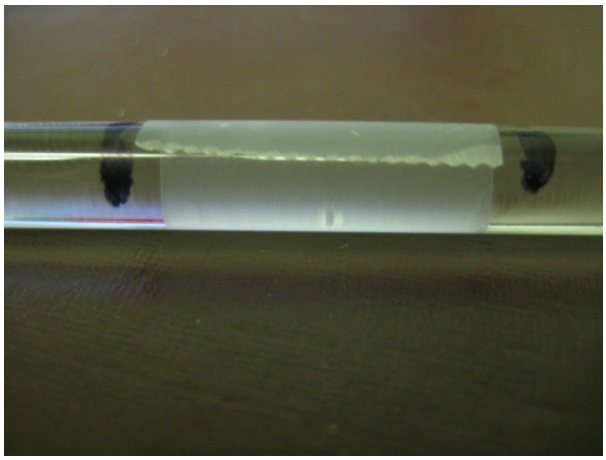

Figure 3.7: An image of a glass rod that has been prepared for fractographic analysis. The black lines mark the volume between loading points and the tape covers the region of compressive stress.

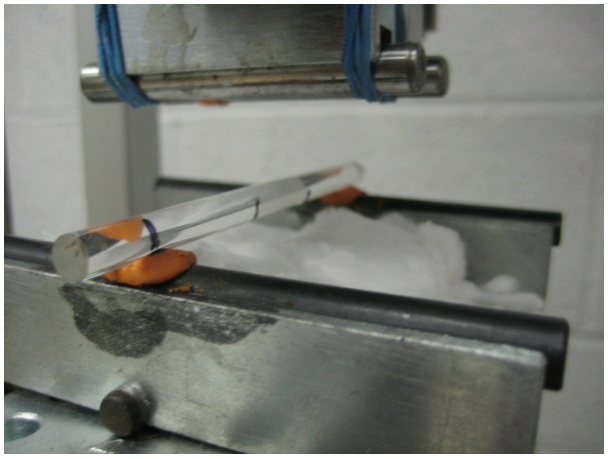

Figure 3.8: An image showing the 4-point bending test setup for a specimen which will be analyzed using fractography.

Immediately after failure, all fragments of the fractured specimen were placed into a labeled sample envelope. This protocol was only used for sample groups which

were to be compared in a fractographic analysis. All other sample groups were prepared using the more simple setup described in the Strength Evaluation section of this chapter.

Prior to conducting any microscopic analysis each specimen was carefully reconstructed and examined to determine the primary fracture and the possible location of a fracture origin. This was done by comparing fracture features with those described in literature[18, 21]. Figure 3.9 shows a fractured specimen which has been reconstructed. The tape is left on the specimen to aid in reconstruction, but also to indicate the region which was under tensile stress (indicating the area in which failure occurred).

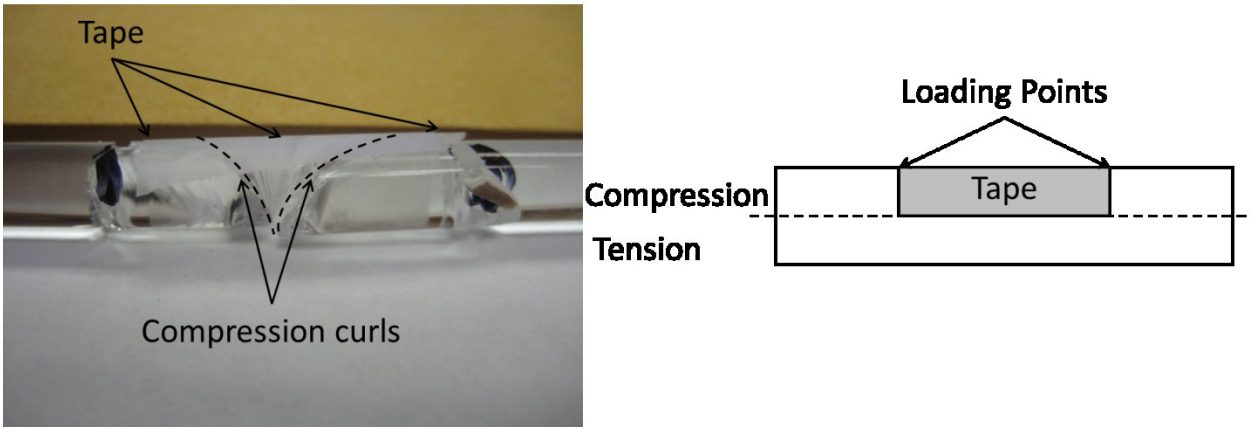


Figure 3.9: A reconstructed specimen which was fractured in 4-point bending (load applied toward the taped region) with compression curls (as shown in Figure 2.11).

An Olympus SZH10 stereo optical microscope capable of 7x magnification was used for close up examination of fracture surfaces. The microscope was fitted with an Olympus QColor-5 5.0 megapixel digital color CCD camera which was used to capture images under magnification. The images were viewed in the QCapture Pro software which can be calibrated to measure image features. A 0.01 mm standard

was used to calibrate the imaging software. Once calibrated the software could be used to measure the sizes of fracture origins and mirror surfaces for each sample.

Fracture mirrors were measured by estimating the epicenter of the fracture along the surface edge of the fracture mirror and making a line to what could be perceived as the edge of the mist region of the fracture origin, as shown in Figure 3.10. Three measurements were taken, each starting at the same epicenter and each extending out to a different part of the semi-circular mist region.

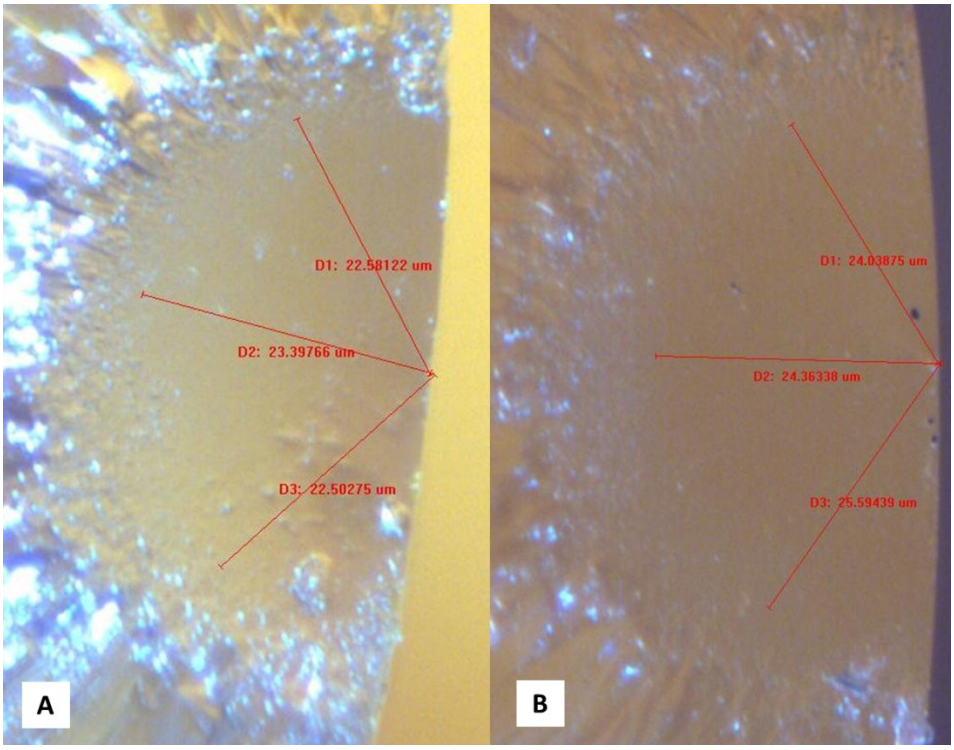


Figure 3.10: Images of the fracture origin at 7x magnification showing three different measurements of the mirror. (A) A glass sample as received, (B) An ion exchanged glass sample. *Note: the sizes of the images have been enlarged.*

**Data Analysis**

The resulting data from the strength evaluations was processed in order to show the effect of the ion exchange process on the variations in strength and reliability of each sample group. The peak load data from the 4-point bending test was converted to Modulus of Rupture data. The average strength and distribution of strengths of each sample group were compared using ANOVA and ***t***-test. The reliability of each sample group was evaluated using a Weibull Analysis.

**Modulus of Rupture (MOR)**

The formulas for the Modulus of Rupture in 4-point bending was adapted from literature to fit the type of specimens being used[20, 22]. The MOR formula for rods in 4-point bending is given in Equation 3.1:

$$\sigma_f = \frac{8P_f(L_1 - L_2)}{\pi D^3}, \tag{3.1}$$

Where,

$\boldsymbol{\sigma_f}$ is the 4-point Modulus of Rupture in megapascals (MPa),

$\boldsymbol{P_f}$ is the load at failure in newtons (N),

$\boldsymbol{L_1}$ is the support span in millimeters (mm),

$\boldsymbol{L_2}$ is the loading span in millimeters (mm), and

$\boldsymbol{D}$ is the diameter of the sample in millimeters (mm).

**Statistical Analysis**

The MOR data gathered from the strength evaluation of each sample group was entered into the JMP 9.0 statistical computer software. JMP was used to calculate the ***F***-test value and confidence interval from a one-way ANOVA; and the ***t***-Test value and confidence interval. The null hypothesis for the ***F***-test in the ANOVA is: All the sample groups being compared are exactly equal. If this is rejected it can be said that *at least* one of the sample groups which was part of the comparison is statistically, significantly different than the other sample groups. The null

hypothesis for the ***t***-Test is: The two sample groups being compared are exactly equal. If this null hypothesis is rejected it can be said that the two sample groups are statistically, significantly different.

Each summary of the analyses which are given by JMP also include a coefficient of determination labeled $R^2$. This parameter is a measurement of how well the linear regression model (used by JMP) fits the data that is being analyzed [23]. An $R^2$ of 1 suggests a perfect fit with the model, where as a value of 0 suggests a poor fit and that there is overwhelming error between the data and the model. Since, as part of this analysis, we are assuming the data fits a normal distribution, this will also give us a measure of how closely that data fits this type of distribution.

**Weibull Analysis**

In practice, the left side of Equation 2.10c is plotted against the natural logarithm of the fracture stress, $\sigma$. From this plot, both the unit volume characteristic strength, $\sigma_0$, and the Weibull modulus, $m$, can be obtained via a linear regression analysis (calculated using Microsoft Excel). The Weibull modulus can be acquired directly as the slope of the linear regression line while the characteristic strength requires a linear interpolation using data from Equation 2.10c.

The linear regression which is used to fit a line to the data also gives an $R^2$ coefficient of determination which has the same meaning as the coefficient of determination given by JMP as part of the statistical analysis [23]. Since the assumption behind this analysis is that the data fits a Weibull distribution, this correlation coefficient can give us a measure of how close this assumption is to actuality.

# Chapter 4: Results and Discussion

## Statistical Analysis

The results shown in Figure 4.1 illustrate the average MOR (calculated using Equation 3.1) of as received and heat treated glass rods over a range of temperatures. The top of each bar represents the arithmetic mean MOR for each sample group, and the range overlaid on each bar indicates one standard deviation from the arithmetic mean of each sample group.

The most important observation to be taken from Figure 4.1 is that there seems to be only a small difference in arithmetic mean MOR between any of the sample groups. In all cases the standard deviations overlap and the arithmetic means only differ by a maximum of 15 MPa between the as received sample group and the sample group heat treated at 200°C. These apparent differences, although small are supported by a statistical analysis as will be shown in Tables 4.1 and 4.2.

These results might have been anticipated due to the low heat treatment temperatures and short exposure times. Also, a slightly lower average strength might be expected for the heat treated sample groups compared to the as received sample group due to increased amount of handling (and thus more chance for new flaws to be introduced to the former).

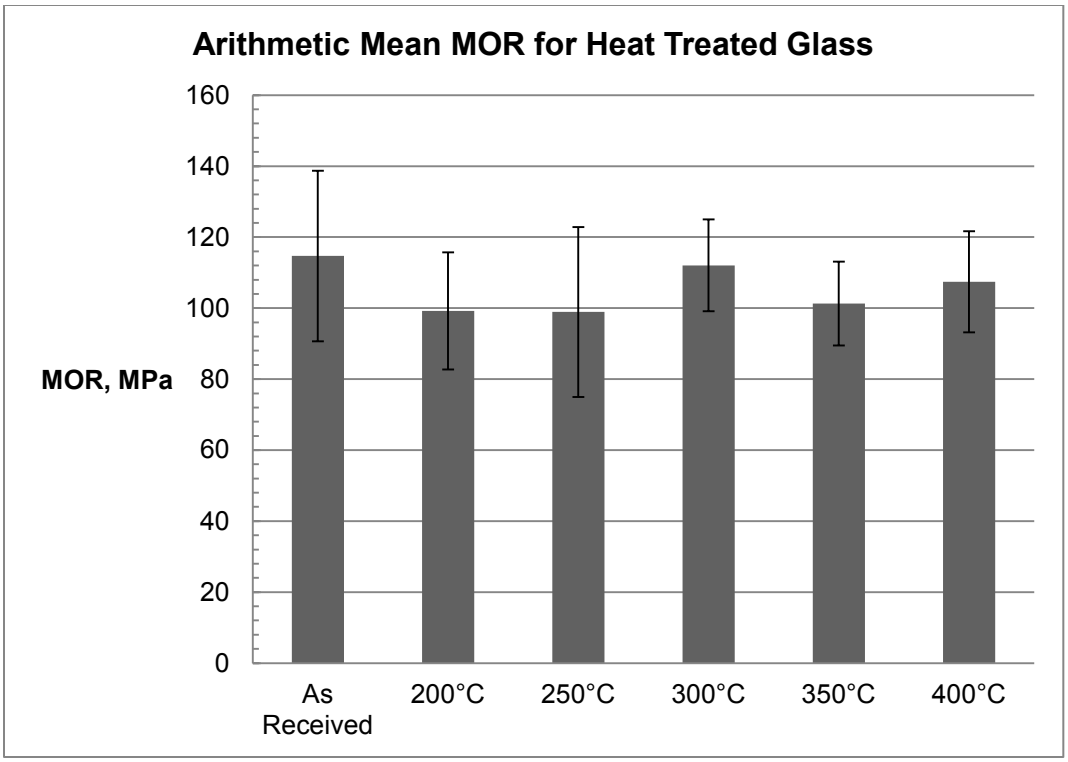


Figure 4.1: An illustration of the average 4-point Modulus of Rupture of sodium borosilicate glass rods as received and heat treated at various temperatures for 15 minutes. The error bars illustrate one standard deviation from the arithmetic mean.

The results in Table 4.1 detail the analysis of variance (ANOVA) between each heat treated sample group and within each heat treated sample group. The probability that the ***F***-statistic is less than the critical ***F***-value was calculated to be 0.0013. This means the null hypothesis, that all of the sample groups have exactly the same distribution of data, is rejected with a 99.87% confidence and *at least* one of the sample groups in the study is different from the rest of the sample groups.

Table 4.1: The ANOVA table summarizes the sources of variance and the results of the F-test for sample groups heat treated at various temperatures.

| **Analysis of Variance for Heat Treated Sample Groups** | | | | | |
|---|---|---|---|---|---|
| **Source** | ***df*** | **Sum of Squares** | **Mean Square** | ***F*-statistic** | **P(*F*-stat < *F*-crit)** |
| Between Samples | 5 | 6938 | 1388 | 4.1695 | 0.0013 |
| Within Samples | 174 | 57975 | 333 | | |
| Total | 179 | 64913 | | | |

The summary of the ***t***-Test results shown in Table 4.2 lead to the same conclusion as the ANOVA. Sample groups which are not connected by the same letter (*A* or *B*) are significantly different (rejecting the null hypothesis) with a confidence of at least 95%. A pairwise analysis of the heat treated sample groups shows that only some of the sample groups have similar distributions of strength while others are statistically different. This illustrates the characteristic scatter which occurs in the strength of glass due to the presence of flaws.

Table 4.2: The summary of ***t***-Test comparison of all heat treated samples with the As Received Samples. Different treatments which are not connected by the same letter (A or B) are significantly different with at least 95% confidence.

| ***t*-Test Result for Samples Heat Treated at Various Temperatures** | | | |
|---|---|---|---|
| **Level** | | | **Least Squares Mean MOR (MPa)** |
| As Received | A | | 115 |
| 300 °C | A | | 112 |
| 400 °C | A | B | 107 |
| 350 °C | | B | 101 |
| 200 °C | | B | 99 |
| 250 °C | | B | 99 |

The coefficient of determination, $\boldsymbol{R^2}$, for the data in Tables 4.1 and 4.2 is 0.11. A value of 1 suggests the data and linear regression model are perfectly fitted. Therefore, this model and data are a poor fit for each other. The Central limit theorem states that the distribution of averages of each sample group must fit a normal distribution with a sample size of 30, but the low value of the coefficient of determination suggests that the distribution of individual strengths within each sample group may not fit a normal distribution.

The average MOR data, calculated using Equation 3.1, shown in Figure 4.2 illustrates the significant increase in strength which occurs as a result of the ion exchange process on glass rods. The increase in strength for glass rods which had

undergone an ion exchange for 15 minutes at 350 °C show an increase in average strength of approximately 125 MPa, and an even greater increase in strength (~180 MPa) for those glass samples which were ion exchanged for 30 minutes at the same temperature. The increase in strength that is shown between the ion exchanged sample groups and those which were only heat treated should also be noted. The range of error overlaid on each bar represents one standard deviation from the arithmetic mean. It should be noted that the standard deviations of the ion exchanged samples have increased substantially as compared with the other sample groups.

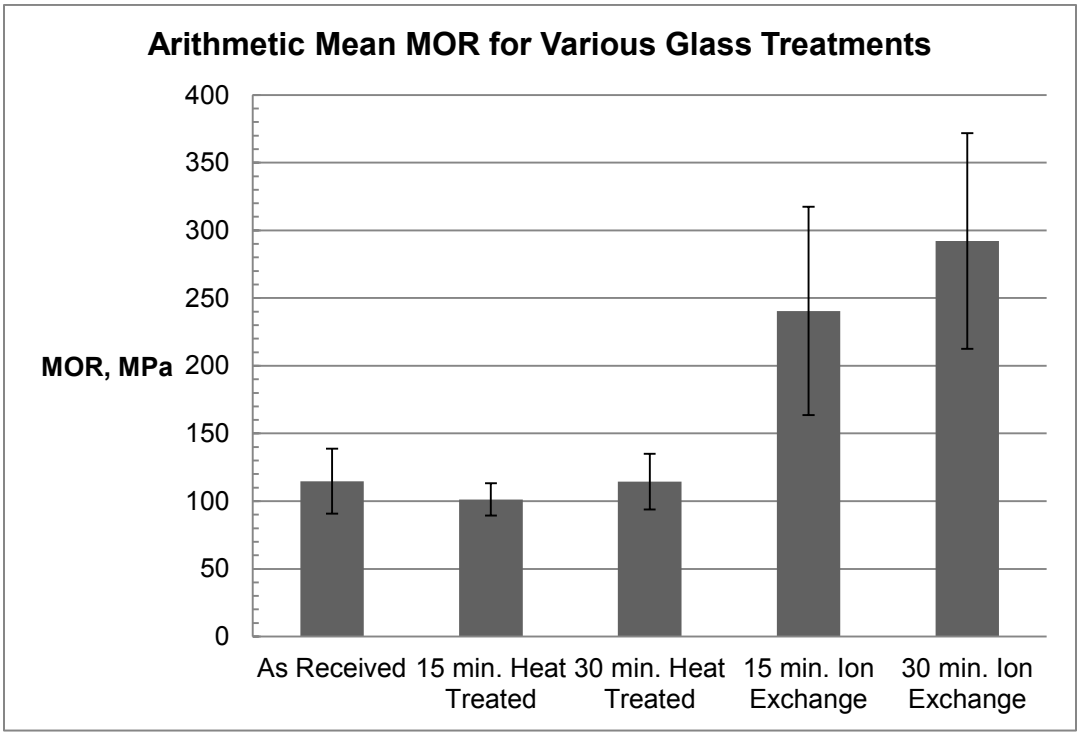


Figure 4.2: A bar graph of the arithmetic average modulus of rupture for sample groups of glass rods after various treatments. The error bars represent one standard deviation from the average. Heat treated and ion exchange treatments were conducted at 350 °C.

A summary of the ANOVA of the MOR for the same sample groups displayed in Figure 4.2 is given in Table 4.3. As in Table 4.1, the focal point of this summary is

the results of the ***F***-test. The probability that the ***F***-statistic is less than the critical ***F***-value is less than 0.01%. This means the null hypothesis, that all of the sample group distributions are exactly the same, is rejected. Thus, it can be stated with 99.9% confidence that *at least* one of the sample groups is different from the others. It is also notable that the variation within sample groups (in the column labeled "Sum of Squares") is of the same order of magnitude as the variation between sample groups. It is likely that this is due to the large variation that exists within the two ion exchanged sample groups.

Table 4.3: A summary of the ANOVA conducted on MOR data resulting from various treatments of glass rod sample groups.

| **Analysis of Variance for Various Treatments** | | | | | |
|---|---|---|---|---|---|
| **Source** | ***df*** | **Sum of Squares** | **Mean Square** | ***F*-statistic** | **P(*F*-stat < *F*-crit)** |
| **Between Sample Groups** | 4 | 922189 | 230547 | 83.1195 | <.0001 |
| **Within Sample Groups** | 145 | 402183 | 2774 | | |
| **Total** | 149 | 1324372 | | | |

A summary of the pair-wise comparison (***t***-Test) of each sample group listed with the other sample groups is given in Table 4.4. Sample groups which are not connected by the same letter (*A*, *B*, or *C*) are considered to have significantly different distributions (rejecting the null hypothesis) with at least 95% confidence. Therefore, the two sample groups treated with the ion exchange process are significantly different from the samples as received and heat treated, as well as being significantly different from each other. This supports the results of the ANOVA in Table 4.3, that at least one of the sample groups is different from the others.

Table 4.4: A summary of the ***t***-Test comparison of MOR data as a result of various treatments of glass rods with As Received samples of glass rods. Treatments not connected by the same letter (A, B, or C) are significantly different with at least 95% confidence. Heat treatments and ion exchange treatments were conducted at 350 °C.

| ***t*-Test Results for Various Treatments** | | | | |
|---|---|---|---|---|
| **Level** | | | | **Least Squares Mean MOR (MPa)** |
| 30 min. Ion Exchange | A | | | 292 |
| 15 min. Ion Exchange | | B | | 240 |
| As Received | | | C | 115 |
| 30 min. Heat Treated | | | C | 114 |
| 15 min. Heat Treated | | | C | 101 |

The statistical analysis of the strength data gathered for each sample group shows that the ion exchange process significantly improved the strength of the glass rods as compared with the glass rods as received and heat treated without an ion exchange bath. The variation within the sample groups as seen in the ANOVA suggests that the ion exchange process may be increasing the width of the strength distribution of the glass rods. The coefficient of determination, $R^2$, for the data in Tables 4.3 and 4.4 is 0.70. A value of 1 suggests the data and linear regression model are perfectly fitted; therefore this model and the data are in moderate agreement with each other. As with the heat treated sample groups (Tables 4.1 and 4.2), a low value of the coefficient of determination for this model suggest that the distribution of the strength of individual specimens in each sample group may not fit a normal distribution.

**Weibull Analysis**

The reliability characteristics of the as received and heat treated glass samples are shown in Figure 4.3 as a probability of failure with increasing stress. The data for all of the sample groups falls within a fairly tight grouping denoting similar characteristic strengths. The characteristic strength, $\sigma_0$, for each data set can be

determined graphically by drawing a line from 63.2% probability of failure on the vertical axis and finding the point on the horizontal axis at which the data set crosses the line. Although it appears from the graph that $\sigma_0$ is the same for all sample sets, small differences become apparent when a linear regression analysis is performed together with linear interpolation using Equations 2.10c. These results can be seen in Figures 4.4 and 4.5. It should also be noted that the slight variations in linear slopes between each data set correlate to variations in the Weibull modulus with changing heat treatment temperature.

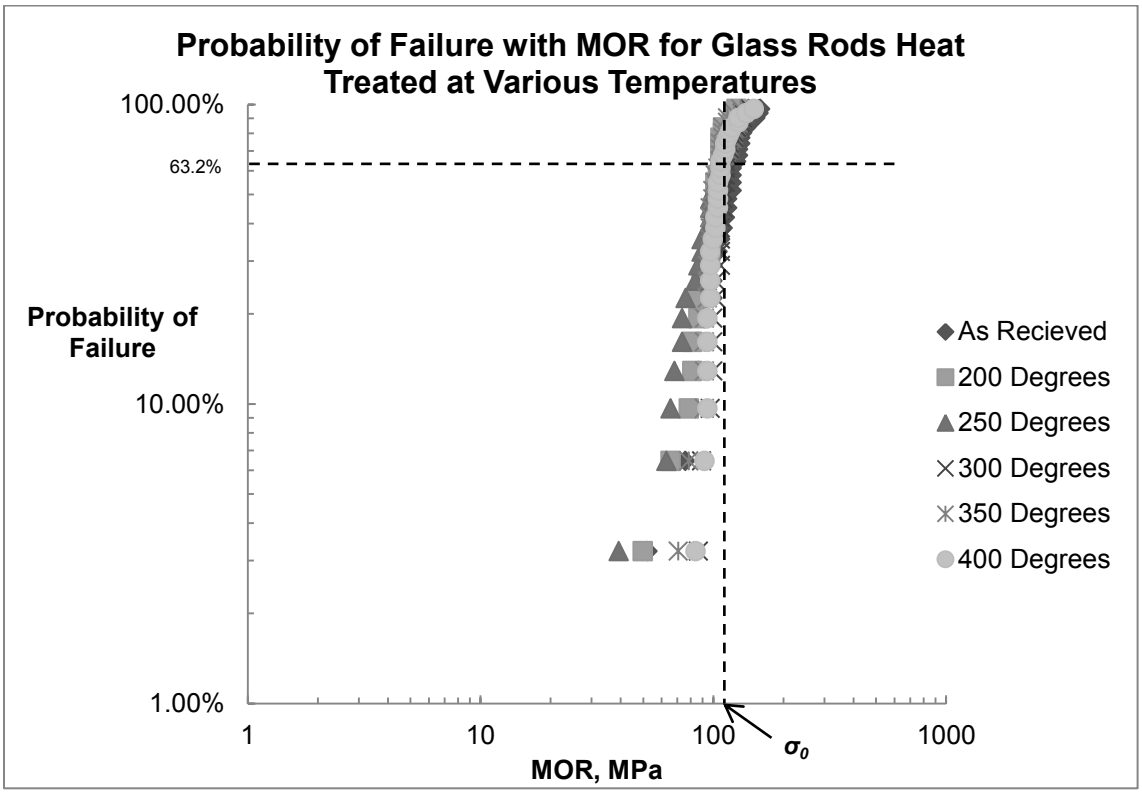


Figure 4.3: This figure illustrates the probability of failure plotted with the modulus of rupture on a logarithmic scale for glass rods heat treated at various temperatures. The dotted lines describe the method of graphically determining $\sigma_0$.

Figure 4.4 illustrates the Weibull modulus, $m$, as it varies with heat treatment temperature and correlates directly to the slopes of the sample groups in Figure 4.3.

The Weibull moduli in this figure were found via linear regression analysis. The error overlaid on each bar describes a 25% expected error above or below the given value of the Weibull modulus (refer to Figure 2.8). The average $\boldsymbol{R^2}$ value for the fitted line used to find these Weibull moduli is 0.93. A value of 1 suggests the linear regression model fits the data sets perfectly. The high value for the coefficient of determination parameter suggests the data fits the Weibull distribution very well. The effects of heat treatment on the Weibull modulus are slightly erratic, but do show a trend toward higher reliability in samples heat treated above 300°C. This trend is most noticeable for data points at lower failure probabilities for samples heat treated at 300 °C and above, as can be seen in Figure 4.3. A lower failure probability denotes samples which failed at a relatively low stress and therefore contained relatively large critical flaws. It should be noticed that these points of low probability of failure shift toward higher values of $\boldsymbol{\sigma}$ with increasing heat treatment temperature while the rest of the data points remain at about the same stress value. This indicates that preferential healing of the cracks may be taking place above 300 °C, but only for those cracks which are relatively large. The shifting of these data points is enough to cause the slope of the distribution to increase, but has only a slight influence on the average strength (one that may be overshadowed by the influence of increased handling as previously discussed).

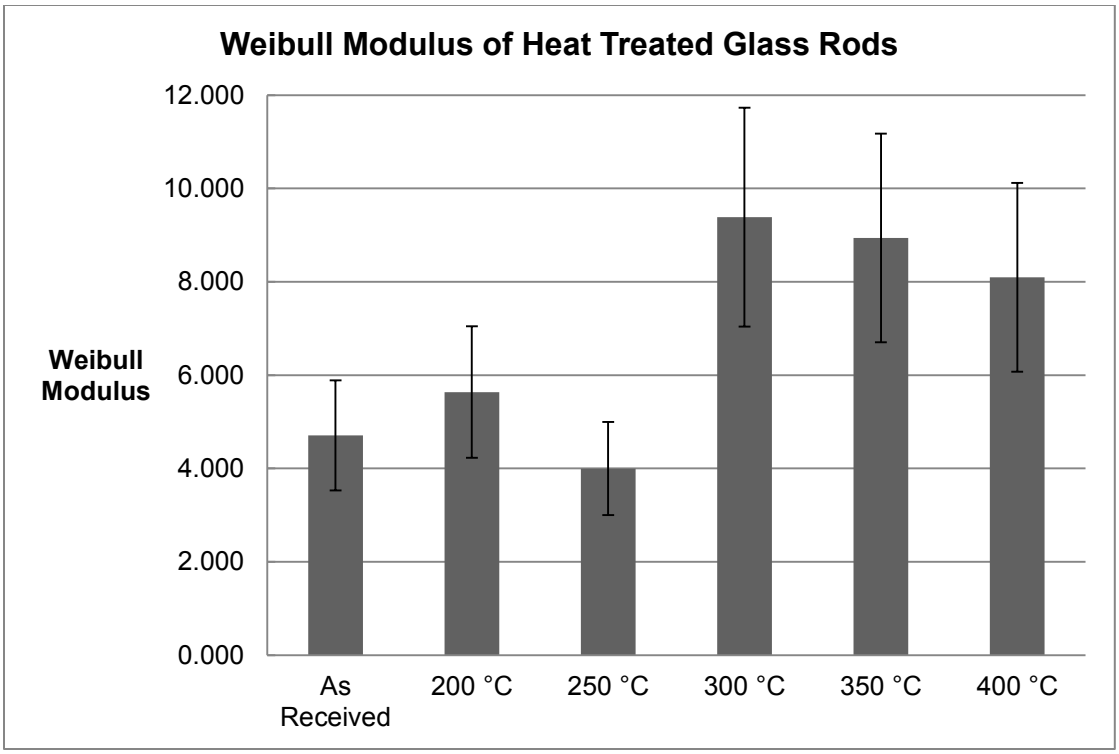


Figure 4.4: A bar graph of the average Weibull modulus as it varies with heat treatment temperature. Heat treatment temperatures were held for 15 minutes. The error bars give a 25% expected error with 90% Confidence (refer to Figure 2.8).

The results of the analysis of the heat treated glass rods' unit volume characteristic strength, $\sigma_0$, in Figure 4.5 are similar to the average MOR results from Figure 4.1. The difference between the as received sample group and 350 °C heat treated sample group, the highest and lowest characteristic strength values, respectively, is approximately 15 MPa. This is the same approximate difference as reported for the average MOR of the glass rods in Figure 4.1. The error overlaid on each bar gives a 5% expected error above or below the given characteristic strength (refer to Figure 2.8). The errors of each sample group overlap, except for the as received. A visual inspection of the of the heat treated samples compared with as received suggests that heat treatment, independent of the temperature, is having a small effect on the strength of the samples.

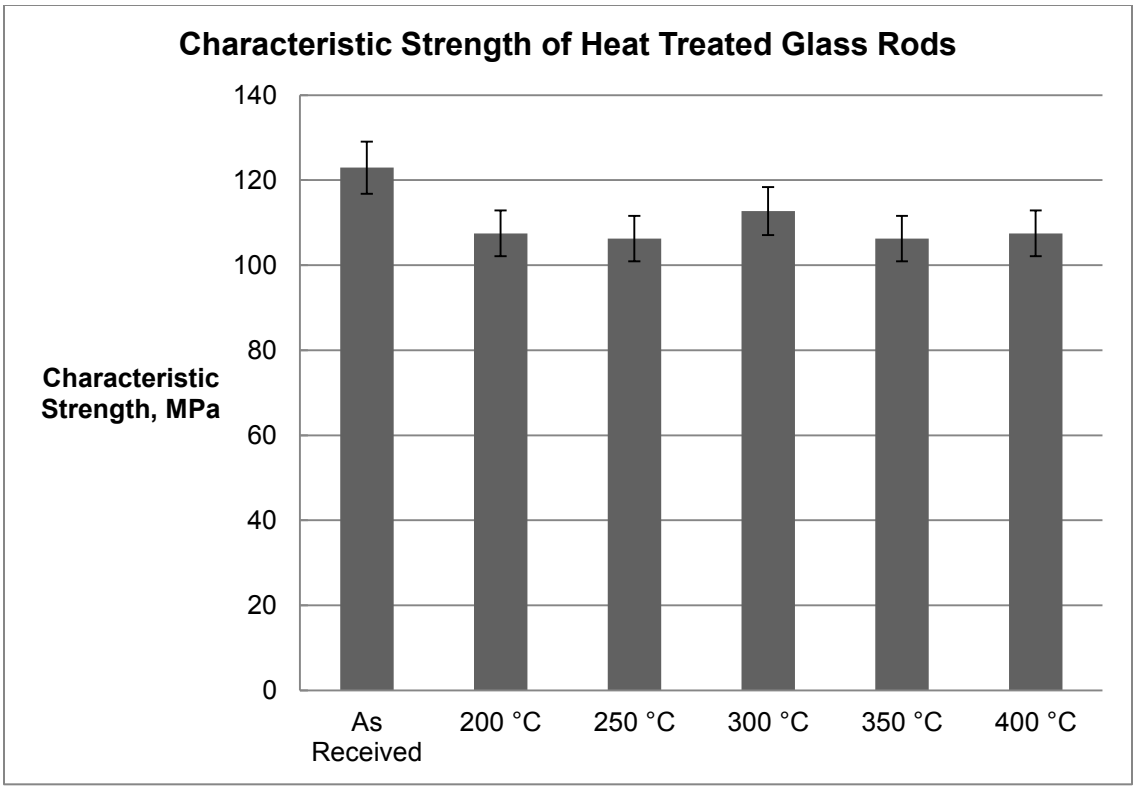


Figure 4.5: A bar graph of the unit volume characteristic strength (calculated using Equation 3.2) as it varies with heat treatment temperature. The error bars represent 5% of the expected error with a 90% confidence interval (refer to Figure 2.8).

The results of the Weibull analysis for the glass rods which were heat treated at various temperatures (shown in Figures 4.4 and 4.5) seem to follow those of the statistical analysis closely. It is interesting to note that the sample groups which were heat treated at 300, 350, and 400 °C have similar characteristic strengths compared to those heat treated at 200 and 250 °C, yet their Weibull moduli were substantially greater. A larger Weibull modulus translates to a smaller flaw size distribution and greater reliability. These data are consistent with the smaller standard deviations shown in Figure 4.1 for the samples heat treated at 300, 350 and 400 °C. Although the reason for this improved reliability is not known it could be related to healing of surface flaws at 300 °C and above [24, 25].

The plots of data in Figure 4.6 illustrate the change in the Weibull characteristics of sample groups which were treated in an ion exchange bath. The ion exchange samples show a decided shift to the right, denoting increased characteristic strength. As in Figure 4.3, the characteristic strength, $\sigma_0$, for each data set can be determined graphically by drawing a line from 63.2% probability of failure on the vertical axis and finding the point on the horizontal axis at which the data set crosses the line. It should also be noted that, although the characteristic strength increases, the Weibull modulus of the data points for the sample group treated in an ion exchange bath for 15 minutes show a noticeable decrease.

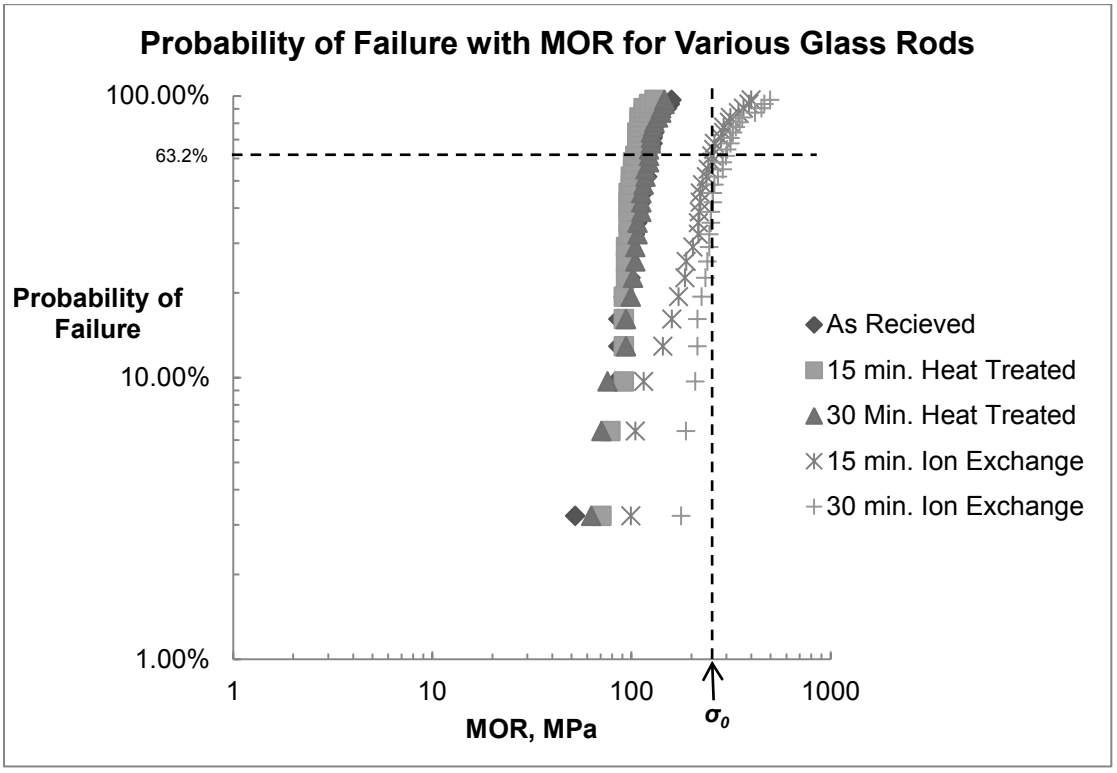


Figure 4.6: A plot of the Probability of Failure as it varies with the modulus of rupture of sample groups of glass rods as a result of various treatments. Heat treatments and ion exchange treatments were conducted at 350 °C. The dotted lines describe the method of graphically determining $\sigma_0$.

The Weibull moduli for the as received, heat treated, and ion exchanged sample groups are shown in Figure 4.7. The overlaid error bars describe a 25% expected error above or below the given Weibull modulus (see Figure 2.8). The average $\boldsymbol{R^2}$ value for the Weibull slopes is 0.94. A value of 1 suggests the linear regression model fits the data sets perfectly. The high value for the correlation of determination suggests the data fits the Weibull distribution very well. The Weibull moduli for the two different ion exchanged sample groups both show a decrease over the as received sample group, with the 15 minute ion exchange distribution resulting in an expected larger decrease. The reason this is expected is that the ion exchange process may not have occurred to as large a case depth as compared to the 30 minute ion exchange. This is evident in Figure 4.6. The data points with lower probabilities of failure for the 15 minute ion exchange sample group only show a small increase in $\boldsymbol{\sigma}$, whereas the same corresponding data points for the 30 minute ion exchange resulted in a significant increase in $\boldsymbol{\sigma}$. A low probability of failure corresponds to a low fracture stress and therefore a large critical flaw size. The tips of the larger critical flaws may have extended past the ion exchange depth of the 15 minute ion exchange sample group. Therefore the residual compressive stress is less effective in reducing the stress at the crack tip. By comparison of Figure 4.7 with Figure 4.4 it is evident that the increase in Weibull modulus that is created by a heat treatment at 350 °C for 15 minutes does not occur when the glass rods are *ion exchanged* at the same temperature for the same amount of time.

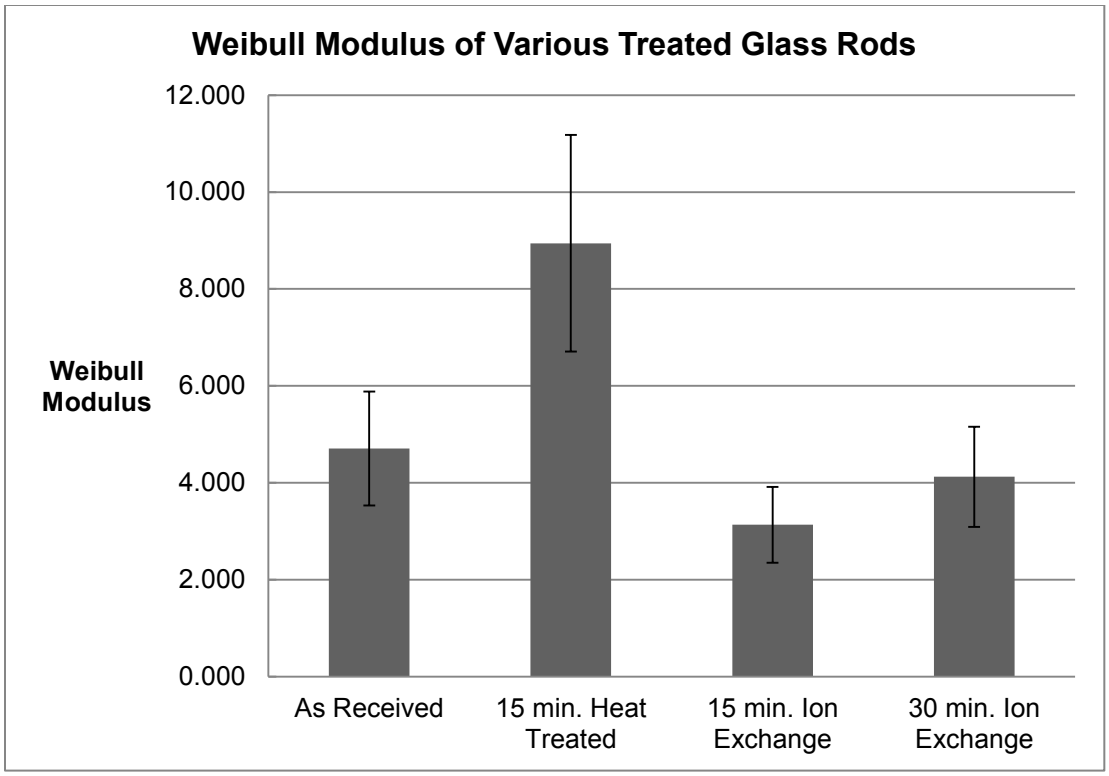


Figure 4.7: A bar chart of the Weibull modulus as it varies with treatment for sample groups of glass rods. The error bars represent a 25% expected error with 90% confidence (refer to Figure 2.8). Heat treatments and ion exchange treatments were conducted at 350 °C.

Figure 4.8 shows a bar chart of the unit volume characteristic strength, $\boldsymbol{\sigma_0}$, as a result of various treatments. The overlaid error bars describe a 5% expected error above or below the given characteristic strength (refer to Figure 2.8). The data from this analysis supports the conclusions drawn from Figure 4.2 and Figure 4.6 that an increase in strength occurred as a result of the ion exchange process. The increase in characteristic strength follows the increase in average MOR closely in that the sample group treated in an ion exchange bath for 15 minutes also shows an approximately 125 MPa increase in characteristic strength. Similarly, the sample group which was ion exchanged for 30 minutes shows an increase in strength of approximately 180 MPa.

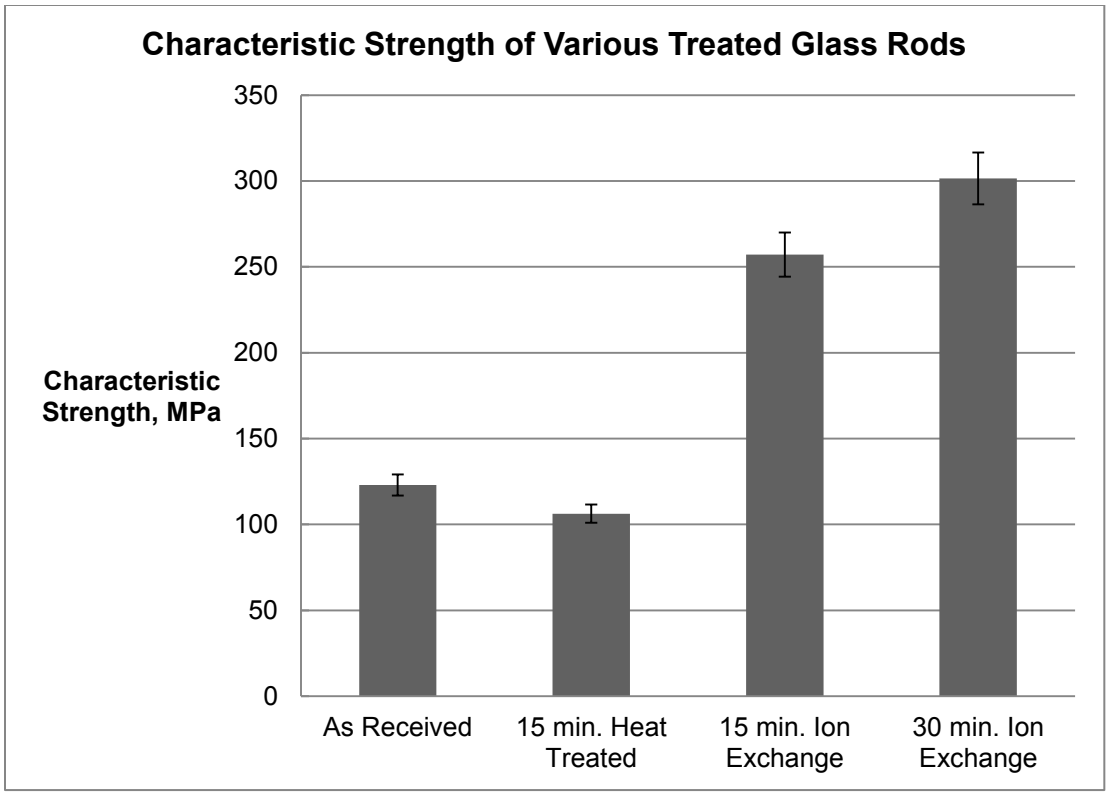


Figure 4.8: A bar chart of unit volume characteristic strength (calculated using Equation 3.2) as it varies with treatment. The error bars represent a 25% expected error with 90% confidence. The heat treatment and ion exchange treatments were conducted at 350°C.

In summary, the Weibull analysis data (in Figures 4.7 and 4.8) shows that the ion exchange increased characteristic strength. In comparison with the as received samples, it can be seen that the Weibull modulus of the ion exchanged samples is about the same as the as received. This is an important finding because it suggests that ion exchange is not significantly affecting the population of flaws. Thus, the increase in strength is most likely due to the induced compressive stress reducing the effectiveness of the flaws in the glass samples as they are received. It should also be noticed that the Weibull analysis has high coefficients of determination, $\boldsymbol{R^2}$. This suggests that using a Weibull analysis to study the variations in the strength of glass is more effective than conducting a statistical analysis (which assumes a normal distribution).

**Fractographic Analysis**

The objective of the fractographic analysis was to determine if fracture surface feature differences exist in glass rods as a result of the ion exchange process. Therefore, the comparison includes an as received sample group and a sample group which has been heat treated in an ion exchange bath at 350 °C for 15 minutes. The sample groups compared in this study are smaller (5 instead of 30) and were prepared separately from those studied in the previous sections of this chapter. However, they were prepared using the exact same methods as described in the experimental methods section.

Visual inspection of Figure 3.10 indicates that both the as received samples and ion exchanged samples have similar fracture morphologies. This suggests that the mechanisms of fracture are not changed as a result of ion exchange strengthening.

Various fracture surface features and strength data are shown in Table 4.5. The critical flaw size was measured on at least one sample of the as received and ion exchanged fracture glasses. These values were used with their respective strengths and Equation 2.2 to determine the fracture toughness (the shape factor was assumed to equal 1). Notice that the fracture toughness of the ion exchanged glass is greater than the as received glass. Once these values were determined, they were used again with Equation 2.2 to determine the critical flaw size (referred to in Table 4.5 as the calculated critical flaw size) for each fractured glass specimen. A comparison of the calculated critical flaw sizes for the two sample sets shows that ion exchange strengthening results in a smaller range of critical flaw sizes (30 to 55 μm) as compared to the as received group (15 to 49 μm). However, the number of samples tested for each group was too small to determine if this difference was

statistically significant. A larger and more detailed study is required to fully understand the significance of these results.

The mirror radii measured from the fracture surfaces are also shown in Table 4.5. Both sample sets yielded similar trends. In general, but not always, the smaller mirror radii corresponded to greater fracture strengths. The ranges of the mirror constants calculated from Equation 2.11 were similar for both groups.

The small number of samples prohibits statistically accurate conclusions. However, from a qualitative standpoint, it can be said that the strength and fracture features of the ion exchanged samples can be described as well with Equation 2.11 as can the as received. In other words the mechanism of fracture is most likely the same for both sample groups.

Table 4.5: The table summarizes the strength and fracture data gathered from the fractographic analysis of as received samples and ion exchanged samples.

| Sample Set | MOR (MPa) | Measured Critical Flaw Size (µm) | Calculated Fracture Toughness (MPa-$m^{1/2}$) | Calculated Critical Flaw Size (µm) | Measured Mirror Radius (µm) | Mirror Constant (MPa-$m^{1/2}$) |
|---|---|---|---|---|---|---|
| As Received | | | | | | |
| 1 | 118 | 30.7 | 0.65 | 28 | 161.2 | 1498 |
| 2 | 105 | | | 35.4 | 228.3 | 1584 |
| 3 | 107 | | | 33.7 | 297.6 | 1855 |
| 4 | 157 | | | 15.7 | 170.3 | 2053 |
| 5 | 89 | 44.4 | 0.59 | 49 | 396.2 | 1774 |
| Average (+/- 1-STD) | 115.4 (22.92) | 37.6 | 0.62 | 32.3 (10.8) | 250.7 (87.57) | 1753 (197.07) |
| Ion Exchanged | | | | | | |
| 1 | 149 | 30.1 | 0.82 | 30.1 | 218.6 | 2209 |
| 2 | 134 | | | 37.6 | 246.6 | 2100 |
| 3 | 142 | | | 33.5 | 137.3 | 1659 |
| 4 | 107 | | | 58.2 | 237.2 | 1655 |
| 5 | 110 | | | 55.4 | 186.5 | 1504 |
| Average (+/- 1-STD) | 128.5 (16.83) | 30.1 | 0.82 | 43 (11.58) | 205.2 (39.7) | 1825 (276.72) |

# Chapter 5: Summary and Conclusion

## Goal and Objectives

The goal of this research project was to investigate the effect that ion exchange had on the variations in the strength of glass rods.

The objectives required for reaching this goal and a summary of how they were satisfied is given below:

1. Develop an ion exchange process which will improve the strength of a commercial sodium borosilicate glass.

   As described in Chapter 3 the time (15 or 30 minutes) and temperature (350 °C) for an ion exchange treatment were chosen; an ion exchange

solution (potassium nitrate) was selected; and a heating schedule and sample handling procedure were developed. A study of the average MOR of glass rods (using sample sets of 30) which were tested as received, heat treated without an ion exchange bath and with an ion exchange bath shows that the ion exchange process described in Chapter 3 did in fact increase the overall strength of the ion exchanged glass rods.

2. Apply methods of statistical analysis to evaluate variations in average strength and the strength distribution due to ion exchange.

   An ANOVA and a ***t***-Test were conducted to evaluate the variations in the strength distributions of both heat treated, and ion exchanged glass rods as compared with the strength distribution of the glass rods as received. In the case of glass heat treated at various temperatures below the annealing point, the results show that while the average strength does not change significantly, the distributions do not remain the same. Statistical analyses of the ion exchanged glass showed that the ion exchange process did in fact have a substantial effect in increasing the entire strength distribution of the glass. However the low values of the coefficient of determination, $\boldsymbol{R^2}$, for the model fitted to the two different sets of data (heat treated and ion exchanged) suggest that a statistical analysis which assumes a normal distribution may not be accurate, this may be because the population that each sample group came from may not be a normal distribution.

3. Conduct a Weibull analysis to investigate variations in characteristic strength and Weibull modulus (reliability) as a result of the ion exchange process.

   A Weibull analysis was conducted on sample groups of glass as received, heat treated, and ion exchanged. Similar to the statistical analyses, the Weibull analysis of the glass rods heat treated at various temperatures below the annealing temperature yielded mixed results. The unit volume characteristic strengths only showed small deviations from the as received sample group, but the Weibull modulus seemed to increase as temperature increased above 300 °C. The reason for this increased Weibull modulus is unknown, but may be related to crack healing. A Weibull analysis of ion exchanged sample groups also yielded similar results to its statistical counterpart. The unit volume characteristic strengths were significantly increased as a result of the ion exchange process, but the Weibull moduli decreased slightly (though maybe not with any statistical significance) as compared with the as received samples. This slight decrease in Weibull modulus of the ion exchange samples may be a result of increased handling (an therefore greater flaw population) from the ion exchange process itself. The Weibull analysis as a whole yielded better coefficients of determination, $\boldsymbol{R^2}$, than its statistical counterpart. This suggests that a Weibull distribution is well fitted for the data collected in this study, and that a Weibull analysis is accurate in describing the variations in the data.

4. Determine, by means of fractography, if similar fracture surface features exist on the glass samples which were treated using ion exchange as on as

received samples, and, if so, determine if these features conform to different models.

Fractography was successfully employed to examine the fracture surface of as received and ion exchanged glass rods. The examination yielded measurements of the fracture mirror radius, and even some measurements of the initial flaw size. The latter allowed the fracture toughness for each group to be calculated. The fracture toughness was greater for the ion exchanged samples. Fracture toughness together with the measured fracture strengths allowed the critical flaw size population to be calculated. These populations were found to be similar for both groups. Further analysis of this data revealed no significant differences between the fracture surface morphology of the as received samples and the ion exchanged samples.

In conclusion, the commercial sodium borosilicate glass can be chemically strengthened. Both statistical and Weibull analyses provide useful information regarding strength variations. However, the Weibull analysis approach provides a better method for predicting the probability of glass fracture under an applied stress. Weibull analysis indicated that at least 30 minutes at 350 °C in molten $KNO_3$ are required to yield effective strengthening results. Fractographic analysis showed that ion exchange does not alter fracture surface features or mechanisms. Taken together, these results suggest that ion exchange does not significantly alter the critical flaw size population but instead reduces the effectiveness of the flaws due to the added compressive stress at the glass surface. Also, while small numbers of test samples should not be used to predict glass strength, analyses of the fracture surface features from these samples still prove useful.

**Future Work**

A similar study should be conducted using the exact glass composition and geometry. However, this study should include greater numbers of samples (at least 50); being sure to conduct a fractographic analysis on all samples of each sample group. The samples should be heat treated at various temperatures (especially including those used in this study) without an ion exchange bath. The goal should be to investigate the effects of heat treatment below the annealing point on the strength variation (especially Weibull modulus), and surface morphology of the glass rods. It may also be worthwhile to experimentally measure the fracture strength of the glass composition being used, so that it can be compared with known and calculated values, as well as be used to calculate the critical flaw to be compared with the measured mirror radius.

Also, a more in depth study similar to this one should be conducted to further investigate the effects of ion exchange on the surface morphology of the glass rods. The ion exchange process should be conducted at various times and temperatures above the molten point of $KNO_3$. Being sure to conduct a fractographic analysis on each sample group, and experimentally measure the fracture toughness after ion exchange. Along with this fractographic analysis a depth profile of the ion concentration would be helpful, especially to compare with fracture mirror radii.

This author suggests that both of these studies focus on the use of a Weibull analysis, but they may also employ statistical analysis techniques as a means of further verification.

# Appendix A

## SCHOTT AR-Glas®
## Physical and Chemical Properties

### Physical Properties

| | | |
|---|---|---|
| Coefficient of mean linear thermal expansion α (20 °C; 300 °C) acc. to DIN ISO 7991 | | $9.1 \cdot 10^{-6}\ K^{-1}$ |
| Transformation temperature $T_g$ | | 525°C |
| Temperature of the glass at viscosity η in dPa · s: | $10^{13}$ (annealing point) | 530°C |
| | $10^{7.6}$ (softening point) | 720°C |
| | $10^{4}$ (working point) | 1040°C |
| Density ρ at 25 °C | | $2.50\ g \cdot cm^{-3}$ |
| Modulus of elasticity E (Young's modulus) | | $73 \cdot 10^{3}\ N \cdot mm^{-2}$ |
| Poisson's ratio μ | | 0.22 |
| Thermal Conductivity $\lambda_w$ bei 90°C | | $1.1\ W \cdot m^{-1} \cdot K^{-1}$ |
| Temperature for the specific electrical resistance of $10^{8}\ \Omega \cdot cm$ (DIN 52 326) $t_{k\,100}$ | | 200°C |
| Logarithm of the electric volume resistivity (Ω · cm) | at 250°C | 7.1 |
| | at 350°C | 5.7 |
| Dielectric properties (1 MHz. 25°C) | | |
| Dielectric constant (permittivity) ε | | 7.2 |
| Dielectric loss factor (dissipation factor) tan δ | | $70 \cdot 10^{-4}$ |
| Refractive index (λ = 587.6 nm) $n_d$ | | 1.514 |
| Stress-optical coefficient (DIN 52 314) K | | $2.7 \cdot 10^{-6}\ mm^2 \cdot N^{-1}$ |

### Chemical Composition

(main components in approx. weight %)

| $SiO_2$ | $B_2O_3$ | $K_2O$ | $Al_2O_3$ |
|---|---|---|---|
| 69 | 1 | 3 | 4 |

| $Na_2O$ | BaO | CaO | MgO |
|---|---|---|---|
| 13 | 2 | 5 | 3 |

### Chemical Resistance

| | |
|---|---|
| Hydrolytic Class (DIN ISO 719) | HGB 3 |
| Acid Class (DIN 12116) | Class S 1 |
| Alkali Class (DIN ISO 695) | Class A 2 |

### Transmission

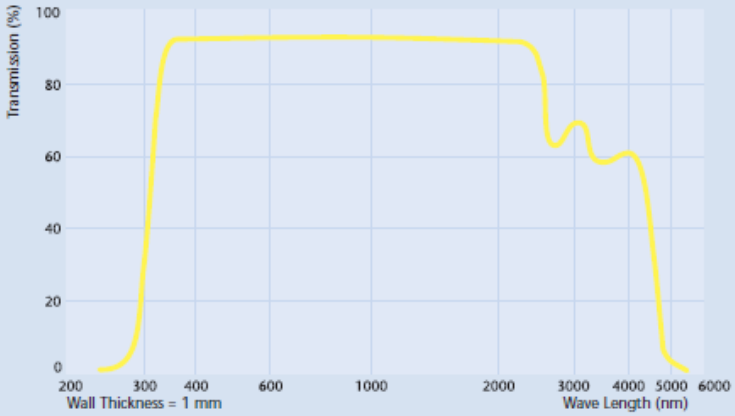


9

## Bibliography


1. Uhlmann, D.R., ed. *Elasticity and Strength in Glasses*. Glass: Science and Technology. Vol. 5. 1980, Academic Press: New York. 218-251.
2. Doremus, R.H., *Glass Science*. 2nd ed. 1994, New York: Wiley. 241-290.
3. Strickland, J. *How Gorilla Glass Works*. 2011 [cited 2012 29 March 2012]; Available from: http://electronics.howstuffworks.com/everyday-tech/gorilla-glass.htm.
4. Mencik, J., *Strength and Fracture of Glass and Ceramics*. Glass Science and Technology. Vol. 12. 1992, Tokyo: Elsevier.
5. Holloway, D.G., *The Physical Properties of Glass*. The Wykeham Science Series, ed. S.N. Mott. Vol. 24. 1973, London: Wykeham Publications.
6. Hammel, J.J. *Some Aspects of Tank Melting*. in *Advances in Ceramics*. 1984. Grossinger, New York: The American Ceramics Society.
7. Inglis, C.E. *Stresses in a plate due to the presence of cracks and sharp corners*. in *Institute of Naval Architecture*. 1913.
8. Griffith, A.A. *The theory of rupture*. in *The First International Congress for Applied Mechanics*. 1924. Delft, Netherlands.
9. Wachtman, J.B., *Mechanical Properties of Ceramics*. 1996, New York: John Wiley & Sons, Inc. 69, 265-267.
10. Frechette, V.D., *Failure Analysis of Brittle Materials*. Vol. 28. 1990, Westerville, OH: The American Ceramic Society, Inc.
11. Varshneya, A.K., *Chemical Strengthening of Glass: Lessons Learned and Yet To Be Learned.* International Journal of Applied Glass Science, 2010. **1**(2): p. 131-142.
12. W.D. Kingery, H.K.B., D. R. Uhlmann, *Introduction to Ceramics*. 1976, New York: John Wiley.
13. Adamson, A.W. and A.P. Gast, *Physical Chemistry of Surfaces*. 1997, New York: Wiley-Interscience.
14. Gaskell, D.R., *An Introduction to Transport Phenomena in Materials Engineering*. 1992, New York: Macmillan. 637.
15. Ott, L., *An Introduction to Statistical Methods and Data Analysis, Second Edition*. 1984, Boston: Dusbury Press.
16. Richardson, D.W., *Modern Ceramic Engineering*. 2nd ed. 1992, New York: Marcel Dekker.
17. McLean, A.F., *Design with Structural Ceramics*, in *Structural Ceramics*, J. John B. Wachtman, Editor. 1989, Academic Press: San Diego, CA. p. 50-63.
18. Quinn, G.D., *Fractography of Ceramics and Glasses*, U.S.D.o. Commerce, Editor 2007, NIST: Materials Science and Engineering Laboratory. p. 546.
19. Bradt, R.C., ed. *Fractography of Glass*. 1994, Plenum Press: New York. 37-74.
20. ASTM, *C158 - 02: Standard Test Methods for Strength of Glass by Flexure (Determination of Modulus of Rupture)*, 2002.
21. ASTM, *C1322 - 05b: Standard Practice for Fractography and Characterization of Fracture Origins in Advanced Ceramics*, 2005, ASTM: West Conshohocken, PA.
22. Jones, J.T., *Ceramics Industrial Processing and Testing*. 2nd ed. 1993, Ames, Iowa: Iowa State University Press.
23. Steel, R.G.D. and J.H. Torrie, *Principles and Procedures of Statistics*. 1960, New York: McGraw-Hill.
24. Michalske, T.A. and E.R. Fuller Jr., *Closure and Repropagation of Healed Cracks in Silicate Glass.* Journal of the American Ceramic Society, 1985. **68**(11): p. 4.
25. Wilson, B.A. and E.D. Case, *In situ microscopy of crack healing in borosilicate glass.* Journal of Materials Science, 1997. **32**: p. 12.